AD-A124 688 ROUGHNESS EFFECTS ON COMPRESSOR OUTLET GUIDE VANES AT HIGH REYNOLDS NUMBE..(U) AIR FORCE INST OF TECH WRIGHT-PATTERSONAAFB OH SCHOOL OF ENGI.. D T GENOVESE

UNCLASSIFIED NOV 82 AFIT/GAE/AA-82D-11 F/G 21/5 NL

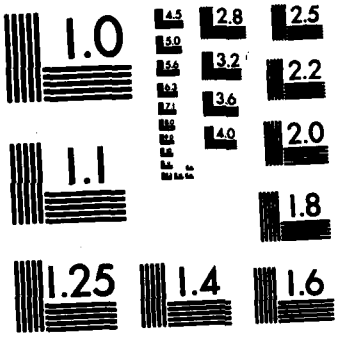

ROUGHNESS EFFECTS ON COMPRESSOR OUTLET GUIDE VANES AT HIGH REYNOLDS NUMBER AND HIGH TURNING ANGLE

THESIS

AFIT/GAE/AA/82D-11 David T. Genovese
Capt USAF

DEPARTMENT OF THE AIR FORCE
AIR UNIVERSITY (ATC)
AIR FORCE INSTITUTE OF TECHNOLOGY

Wright-Patterson Air Force Base, Ohio

AFIT/GAE/AA/82D-11

ROUGHNESS EFFECTS ON COMPRESSOR OUTLET GUIDE VANES AT HIGH REYNOLDS NUMBER AND HIGH TURNING ANGLE

THESIS

AFIT/GAE/AA/82D-11 David T. Genovese
Capt USAF

AFIT/GAE/AA/82D-11

ROUGHNESS EFFECTS ON COMPRESSOR OUTLET GUIDE VANES AT HIGH REYNOLDS NUMBER AND HIGH TURNING ANGLE

THESIS

Presented to the Faculty of the School of Engineering

of the Air Force Institute of Technology

Air University

in Partial Fulfillment of the

Requirements for the Degree of

Master of Science

by

David T. Genovese, B.S.

Capt USAF

Graduate Aeronautical Engineering

November 1982

Preface

I would like to express my thanks to my advisor Dr. William C. Elrod and to the members of my committee Dr. Peter J. Torvik and Dr. Harold E. Wright for their guidance through a unique sense of direction, purpose and perspective which was invaluable to me during the effort discussed on the pages to follow. I am very appreciative of the help given to me by Major John Vonada on my investigation through his constant efforts on the Cascade Test Facility which made it the tool for research it is today. I would also like to thank Mr. Gregory B. Tibbs for his much needed assistance. The the tried and true support of the AFIT Fabrication Branch along with the backing of Mr.William Baker and Mr. Harold Cannon of the Department of Aeronautics and Astronautics was also a welcome addition to my effort.

David T. Genovese

CONTENTS

List of Figures

List of Symbols

c	Chord	in
Cd	Section coefficient of drag	
cv	Cut-off value	micro-in
D	Drag	lbs
L	Roughness sample length	micro-in
Ra	Arithmetic average roughness	micro-in
Rtm	Average maximum peak to valley dimension	micro-in
Rtmax	Maximum peak to valley dimension	micro-in
S	Area	sq-in
V	Velocity downstream of cascade	ft/sec
Vo	Inlet velocity to cascade	ft/sec
v	Distance from centerline	micro-in
ρ	Density	lb/cubic-ft

List of Tables

Abstract

An experimental investigation of the effects of surface roughness on flow at high Reynolds number over compressor outlet guide vanes at high turning angle in a 2-D cascade was conducted at the Air Force Institute of Technology Cascade Test Facility. A NACA 64 Series airfoil with a design lift coefficient of 0.9 and a thickness of 5.5 percent was tested at a solidity of 1.5 and a 27 degree angle of attack.

Two models of roughness were tested: one smoother and one rougher than actual compressor vanes. Four configurations of roughness were evaluated: pressure and suction sides smooth, pressure and suction sides rough, pressure side rough with the suction side smooth and suction side rough with the pressure side smooth.

Hot film sensor anemometry was used to determine the velocity and turbulence intensity in the flow field behind the vanes. The section coefficient of drag was calculated based on momentum deficit theory.

Roughness was determined to effect the flow through an increase in the coefficient of drag and changes to the magnitude and profiles of the velocity and turbulence intensity. The greatest effect was caused by roughness on the suction side of the vane with a smooth pressure side.

I. Introduction

Background

The need for increased turbine engine efficiency of operation along with reduced manufacturing and maintenance time has become of prime interest within the aerospace industry due to recent escalation of fuel and labor costs. The Air Force usage of aviation fuel is in excess of 3.6 billion gallons each year at a cost of over 5 billion dollars. Maintenance manhours resulting in the expenditure of hundreds of millions of dollars added to this cost produce a situation where a small percentage of saving can result in large returns.

The aircraft turbine engine compressor is a key component where there is potential for significant savings resulting from small increases of efficiency. Determination of the effects of compressor blade and vane surface roughness on engine performance would provide a basis for increased efficiency of operation with resultant cost savings brought about by the reduction of fuel consumption. Additionally, surface finish requirements directly affect the initial manufacturing standards of these components while also establishing the ammount of overhaul and maintenance needed.

The establishment of a technically substantiated surface finish requirement for compressor blades and vanes is critical to the realization of both optimized engine

performance and efficient labor utilization. This can only be achieved once the effects of roughness on the flow are quantified.

Objectives and Scope

The objective of this investigation was to determine roughness effects on the performance of compressor outlet guide vane airfoils at high turning angle in flow with a Reynolds number in excess of one million. A NACA 64 series airfoil with a design lift coefficient of 0.9 and a thickness of 5.5 percent was tested in a two-dimensional cascade with a solidity of 1.5 at 27 degrees angle of attack.

Two different orders of surface roughness were tested in four configurations: pressure and suction sides smooth, pressure and suction sides rough, suction side rough with pressure side smooth and pressure side rough with suction side smooth.

The method of investigation was to measure the flow velocity behind an airfoil in the cascade with a hot film anemometer sensor and calculate the turbulence intensity. The velocity profile was then used to calculate the coefficient of drag based on the momentum deficit in the flow brought about by the airfoil.

The figures of merit chosen to evaluate the effects of roughness on the flow were the section coefficient of drag along with the velocity and turbulence intensity profiles.

II. THEORY

Momentum Deficit and Profile Drag

The theory of wake survey measurement provides that air flow past an airfoil experiences a loss in momentum which is equal to the profile drag of that airfoil. This is expressed mathematically by:

$$D = \int_A \rho V (V_o - V)\, dA \qquad (1)$$

where D is drag, Vo is initial airspeed in front of the airfoil, V is the airspeed at an observation point in the wake, and dA is defined as a small area of the wake perpendicular to the airstream (Ref 9:165-168). The drag may be converted to the coefficient of drag through the following relation:

$$C_d = \frac{D}{\rho/2 V_o^2 S} \qquad (2)$$

where S is the area of the airfoil. This relation may be reduced to one dimension by assuming a unit section of airfoil for which S=Chord x 1 and dA=dy as expressed by:

$$C_d = \int \frac{2}{C}\left(\frac{V}{V_o} - \frac{V^2}{V_o^2}\right) dy \qquad (3)$$

Substitution of the value for the chord length of 2 inches reduces the relation for the section coefficient of drag to the

final form of:

$$C = \int \left(\frac{V}{V_o} - \frac{V_o^2}{V_o^2} \right) dy \qquad (4)$$

This integral may be numerically evaluated across the data plane with dy as the step size in the y direction using Simpsons Rule (Ref 1:148-151).

The drag coefficient is a figure of merit for a given airfoil and may be used to evaluate the effects brought about by surface roughness.

Surface Roughness and Model Definition

Surface roughness, the technical definition of surface texture, is defined as the finer irregularities in the repetitive or random deviations from an intended surface contour (Ref 2:2). This constitutes a series of peaks and valleys along the surface. The overall order of these peaks and valleys is expressed as the arithmetic average roughness, Ra, as defined by:

$$R_a = \frac{1}{L} \int |y| \, dx \qquad (5)$$

where Ra is the arithmetic average deviation from the intended surface contour, y is the height above or below the centerline, and L is the sampling length. Figure 1 illustrates the basis of arithmetic average roughness (Ref 2:3).

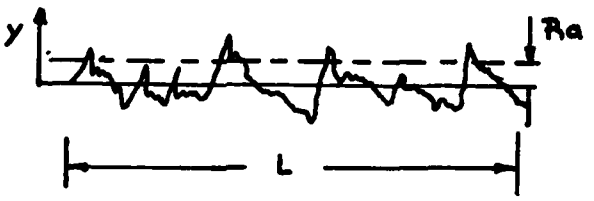

Figure 1. Arithmetic average roughness

Although a valuable measurement parameter, arithmetic average roughness, of itself, does not adequately define the hydrodynamic character of a surface (Ref 3:10). Fluid flow across a surface with a given roughness is most affected by the largest of the peaks and valleys.

Further definition of the surface character is given by the measurement of the average of the maximum peak to valley measurements for a series of given lengths along a surface as shown in Figure 2. This measurement, refered to as Rtm, provides a more accurate measure of the hydrodynamic character of a surface (Ref 3).

A definitive evaluation of surface texture results from the measurement of the arithmetic average roughness Ra, in conjunction with the average of the maximum peak to valley measurements,Rtm. The calculation of Rtm (through the use of equation 6) makes use of data from the roughness trace as illustrated in Figure 2 (Ref 4).

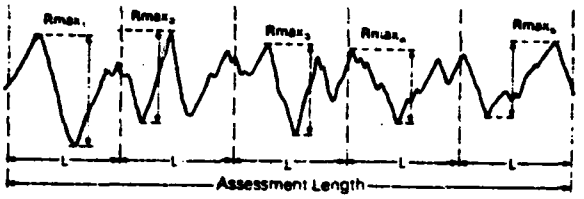

Figure 2. Rtm

$$R_{tm} = \frac{R_{max1} + R_{max2} + R_{max3} + R_{max4} + R_{max5}}{5} \quad (6)$$

It can be seen that this parameter is calculated from values of the maximum peak to valley distance for each of five lengths along the surface.

The combination of arithmetic average roughness,Ra, and Rtm, the average maximum peak to valley dimension, define the characterization of hydrodynamically effective surface roughness in this investigation.

A baseline surface character was determined from a survey of actual compressor blades and vanes. The measurement of arithmetic average roughness correlated well with the survey of Stiles (Ref 2). Further definition of the surface character was performed through measurement of the parameter Rtm.

With this known surface definition of actual vanes, test vanes were made both smoother and rougher by a considerable degree. Table I presents the results of the surface characterizatons of the baseline, smooth and rough vane surfaces. There are obvious differences in the magnitudes of

the roughness parameters between the three surface models.

Comparison of the smooth vane model with the vane and blade surfaces surveyed by Stiles reveals that the smooth vanes tested in this investigation were smoother than any blades or vanes of either new or used condition. This was desired to provide as absolute as possible a set of data for the purpose of determining the effects of roughness on blade performance in the cascade.

The rough vanes tested were of the same order as the roughness of used blades and vanes from actual compressors. The smooth and rough vane surfaces used for this investigation effectively bracketed the actual vane surfaces in the measurement of Ra and Rtm.

A qualitative analysis of surface texture was performed through tracing the surfaces of the baseline, smooth, and rough vane surfaces. Figure 3 presents representative traces of the three surfaces.

The smooth vane surface can be seen to be both smoother and more uniform than the baseline vane surface. These qualities provide a less hydrodynamically distrubing surface to the flow. The rough vane surface is both considerably rougher and more random than the baseline vane. This produces a surface which is more hydrodynamically disturbing than either of the other two surfaces.

TABLE I

MODEL SURFACE CHARACTERIZATION

	Ra (micro in)	Rtm (micro in)
SUCTION SIDE		
Chordwise Measurement		
Smooth	3	27
Baseline	14	130
Rough	96	682
Spanwise Measurement		
Smooth	4	33
Baseline	12	119
Rough	74	554
PRESSURE SIDE		
Chordwise Measurement		
Smooth	4	25
Baseline	18	164
Rough	97	618
Spanwise Measurement		
Smooth	4	24
Baseline	16	130
Rough	55	416

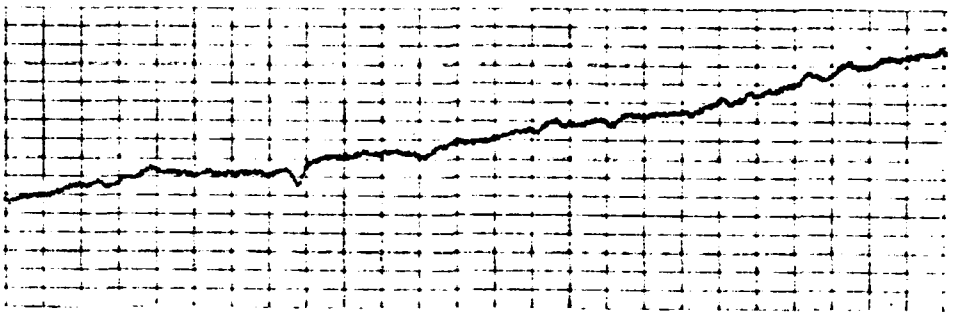

(a) Smooth Vanes: Vertical Scale 10000X, Horizontal Scale 200X

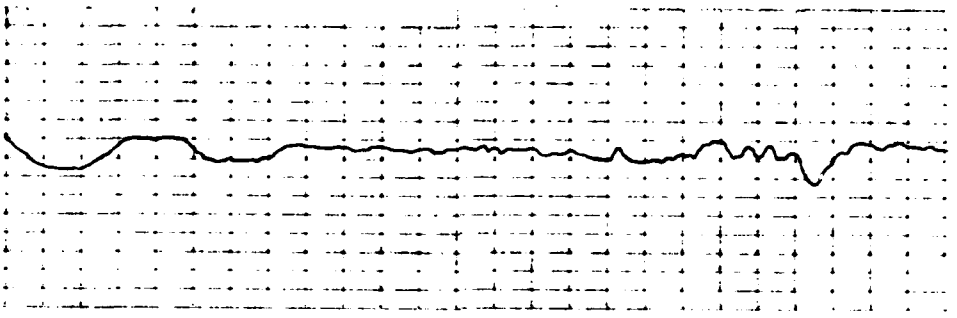

(b) Baseline Metal Vanes: Vertical Scale 2000X, Horizontal Scale 200X

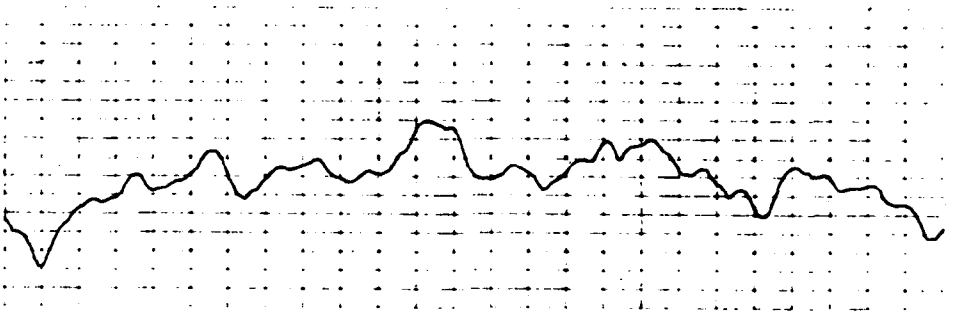

(c) Rough Vanes: Vertical Scale 2000X, Horizontal Scale 200X

Figure 3. Surface Traces.

III. EXPERIMENTAL EQUIPMENT AND METHOD

Cascade Test Facility

The Cascade Test Facility at the Air Force Institute of Technology School of Engineering was used for this investigation. This facility consists of a flow supply system coupled to a diffuser/stilling chamber which provides flow at Reynolds number in excess of one million per foot to a 16 square inch test section as reported in detail by Allison (Ref 5).

Source air was filtered through an electrostatic cleaner in combination with a series of fiber filters after which it was conditioned by a flow straightner before entering the test section. The facility provided an air supply with adequate cleanliness and turbulence intensities on the order of 1 percent for the purpose of hot film sensor anemometry investigation of flow fields.

Test Section

The test section was designed as a two-dimensional outlet guide vane cascade containing 7 NACA 64 series airfoils with a design lift coefficient of 0.9 and thickness of 5.5 percent. The 2 inch chord by 2 inch width vanes were made from casting epoxy.

The testing configuration was specified by an aspect ratio of 1.0, a solidity of 1.5 and a vane angle of attack of

27 degrees. The vane spacing was 1.333 inches.

A computer controlled traverser was used to position the hot film sensor probe support in the flow. Data was taken in a plane perpendicular to the flow direction at each of 5 locations behind the center blade. These data planes correspond to locations along the flow of .125, .625, 1.125, 1.625, and 2.125 chord lengths(c=2inches). Figure 4 illustrates the test section setup and the data plane locations.

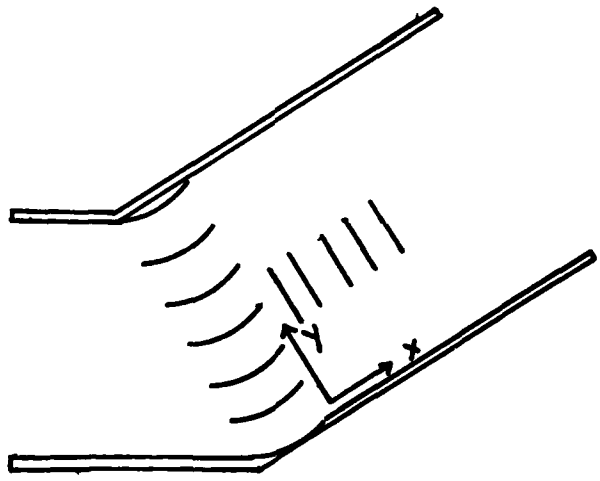

Figure 4. Test Section and Data Planes

One hundred data points were taken along each plane at a spacing of .01 inches in the Y-direction. This provided a survey of both the free stream and vane wake flows.

Instrumentation

A TSI model 1241-10 End Flow hot film sensor operated by two TSI model 1050 Constant Temperature Anemometers was used to survey the flow field. Velocity and turbulence intensity in both the X and Y directions were obtained. The test section inlet velocity was calculated based on the stilling chamber total temperature and pressure along with the static pressure at the inlet to the cascade as measured by thermocouples and pressure transducers. Free stream mean velocity was calculated based on the stilling chamber total pressure and temperature along with the static pressure measured at each of the five data planes. These static pressures were measured from ports along the side walls of the test section. All velocities calculated were based on assuming a condition of incompressible isentropic flow.

The use of stilling chamber total pressure was based on a pressure survey of the flow field in the test section. The difference between the actual total pressure and the chamber total pressure was determined to be less than one half of one percent. This resulted in an error in the calculation of the velocity of less than 0.1 percent.

Data Acquisition and Processing

Data acquisiton, management and reduction were all performed by a computerized data acquisition system integrated into the Cascade Test Facility (Ref 7). The data acquisition

system and constant temperature anemometers were located in an environmentally controlled room adjacent to the Cascade Test Facility. The controlled environment was necessary to reduce the effects of ambient temperture fluctuations on the resistance of the bridge circuit of the anemometer.

The computer system directed the traverser to each discrete data location and used a scanner to step the voltmeter through the channels to record all output from the anemometers, thermocouples, and pressure transducers. The digitized voltage measurements for each test were stored in core then written onto magnetic storage discs. These voltages were later converted to velocities, pressures, temperatures and turbulence intensities along with other performance indicators. The reduced data was printed out in a format as indicated in Appendix A. All plots were done on a graphics plotter integral to the system.

Hot Film Sensor Calibration and Correction

The hot film sensor was calibrated using a temperature compensation routine developed by Rivir and Vonada (Ref 6; Ref 7). This compensation corrected for variations in the heat transfer of the sensor resulting from changes in fluid temperature which caused an error on the order of 5 percent in measured velocity (Ref 10). Accuracy to within 5 to 7 percent error was attained using this correction.

This remaining error was caused by uncontrollable

variations in test section air humidity (Ref 8). A further correction to the velocity measured by the hot film sensor was performed based on the free stream velocity in the flow field. A pressure survey test was performed at each of the data planes using a total pressure probe. Flow field velocities were calculated using the measured total pressure along with the total temperature of the stilling chamber and the wall static pressure for each data plane. A successive test, under the same conditions, was then performed using a hot film sensor. The velocities measured by the hot film sensor and derived from the total pressure at each point in the free stream were then compared. A correction factor was defined as the difference between the velocity measured by the hot film sensor and the total pressure probe derived velocity with the total pressure probe derived velocity assumed correct. As indicated above, the stilling chamber total pressure may be used with the data plane static pressure to determine the velocity with very small error. Therefore, use of the chamber total pressure permitted calculation of the correction factor for each data point to adjust the velocity measured by the hot film sensor. This allowed a continuous check on the integrity and reliability of the velocity measured by the hot film sensor. Correction of the velocity in this manner was effective in reducing the errors of measurement induced by humidity to less than one half of one percent.

Roughness Models

A baseline survey of actual compressor blades and vanes was used to establish the surface character of operational components (Ref 2). Two roughness models were used for the experimental investigation; one significantly smoother and one significantly rougher than the blades and vanes found in actual compressors. In order to simulate roughness on the test vane surfaces, the vane specimens were sanded with 80 grit sandpaper, first in the chordwise, and then in the spanwise direction. This produced a surface which exibited a character which would have a definite hydrodynamic effect on the flow over the vanes based on the values of Ra and Rtm. Smooth surfaces were created through polishing the mold used for casting of the vanes.

Four configurations of surface roughness were tested: smooth pressure and suction sides, roughness on both the pressure and suction sides, roughness on the pressure side with a smooth suction side, and roughness on the suction side with a smooth pressure side. These configurations were chosen to determine the effect of roughness relative to a baseline of a smooth configuration under the operating conditions of high Reynolds number and high turning angle.

Profilometer and Surface Measurement

Surface roughness was measured with a Rank Taylor Hobson Surtronic 3 Profilometer in combination with Parameter and Recorder Modules. A variable reluctance pick-up with a 200 micro inch tip radius diamond stylus was used for all work for this investigation. Measurements were made of arithmetic average roughness,Ra, and average peak to valley dimension,Rtm. In addition, traces of the actual surface were made.

Both the pressure and suction sides were surveyed in the chordwise and spanwise directions at 50 percent span and each of 25, 50, and 75 percent chord. A measurement sample length,L, of 0.01 inches was used and all measurements were recorded in micro inches. Twenty five points were taken at each location for a total of 300 data points for each vane in order to determine the surface character of each test vane.

Performance Evaluation

Evaluation of the effects of surface roughness was based on the calculation of the coefficient of drag of the various airfoil sections along with an evaluation of the velocity and turbulence intensity profiles of the flow field. These factors were considered to indicate the relative effects of roughness with respect to the performance of a baseline of vanes with smooth pressure and suction surfaces.

IV. EXPERIMENTAL RESULTS AND DISCUSSION

Two models of compressor vane roughness were selected to determine the effect of surface roughness on vane performance in cascades. These models were tested in a total of four configurations: both sides smooth, both sides rough, pressure side rough with the suction side smooth, and suction side rough with the pressure side smooth.

The coefficient of drag along with the velocity and turbulence intensity profiles were chosen to evaluate the effects of surface roughness on the flow field for this investigation.

Velocity and Turbulence Intensity Profiles

The velocity and turbulence intensity data for all tests was plotted for the five data planes, each of which corresponds to one traverse of the flow field at a position downstream from the vane trailing edge. The plotted velocity values were non-dimensionalized by dividing the measured velocity at each data location by the velocity at the cascade inlet. These values were then multiplied by 550 feet per second to allow an easy comparison of the data obtained for the various configurations investigated. This procedure was chosen to eliminate the effects of small changes in ambient temperature and pressure which occured from test to test and resulted in changes of the inlet velocity to the cascade.

The resulting velocities for each of the 100 data points

at each traverse plane were plotted as a means of comparing the effects of different vane surface roughnesses. These plots reflect both the X and Y components of velocity which have been resolved into vectors representing the magnitude and direction of the flow at the given data point. The origin of the vector is the point at which the data was measured while the direction and length represent the actual flow magnitude and direction when interpreted through use of the scale factor for the representative plot.

The turbulence intensity was calculated from the rms X and Y components of the dynamic velocity through use of the following relation:

$$\text{Turbulence Intensity} = \text{rms Velocity}/\text{Mean Velocity} \qquad (7)$$

These values were plotted on the same figures as the velocity profile vectors with the origin as the data point location and the magnitude and direction representative of the values measured when interpreted with the proper scale factor. This format of presentation allowed a comparison between the velocity values and the respective turbulence intensity for both the individual data points and the flow field in general.

A small shift of the velocity decrement toward the positive Y direction is evident at stations farther downstream from the vane trailing edge for all plotted data. This is a result of a 3 degree misalignment of the probe

traverser with respect to the actual flow direction. The result is a shift of the point at which data is taken in the flow at stations farther downstream from the trailing edge of the vane. It should be noted that this shift is not a product of any changes in the flow direction, but merely a change in the location of data measurement which does not affect the results in any way when interpreted appropriately.

The results of the smooth vane test are presented in Figure 5. These five plots display the velocity and turbulence intensity profiles for each of the five data planes investigated. An obvious velocity deficit is visible with a high initial decay rate which reduces further along the flow as evidenced through comparison of plots 5a through 5e. High turbulence intensities can be seen in the wake directly behind the vane trailing edge. These levels reduce at each successive traverse at locations farther downstream from the vane trailing edge. Both the velocity decrement and turbulence intensity contours are narrow and pronounced at the initial traverse. These levels are reduced and become consistently broader at stations farther downstream from the vane trailing edge.

A verification of repeatibility was performed using the smooth vanes. This was done by running a second test of the same vanes and comparing the velocity and turbulence intensity profiles. The section coefficient of drag was also calculated for both tests. The results of the second test were to within less than one half of one percent of

difference with respect to the initial smooth vane test. The velocity and turbulence intensity profiles for the repeatibility test are presented in Appendix B.

The results of the test with roughness on both sides of the vanes are presented in Figure 6. The same characteristic turbulence intensity and velocity deficit and decay behavior in the wake of the vane are exibited as were seen for the smooth vanes. However, the level of free stream turbulence intensity increases significantly at stations farther downstream from the vane trailing edge while the region of turbulence in the wake becomes progressively wider.

Figure 7 presents the results of the test of vanes with roughness on the pressure side of the airfoil along with a smooth suction side surface. The behavior of the velocity is similar to that of the smooth vanes (Fig 5). The free stream turbulence intensity remains at the same level throughout the flow, whereas the wake region turbulence intensity broadens on the suction side while progressing to stations farther downstream from the vane trailing edge.

Figure 8 presents the results of the test of vanes with a rough suction side surface along with a smooth pressure side surface. A shift of the flow towards the pressure side can be seen at stations farther downstream from the vane trailing edge. The level of free stream turbulence remains constant along the flow direction while there is a broadening of the turbulence intensity on the suction side in the near wake region.

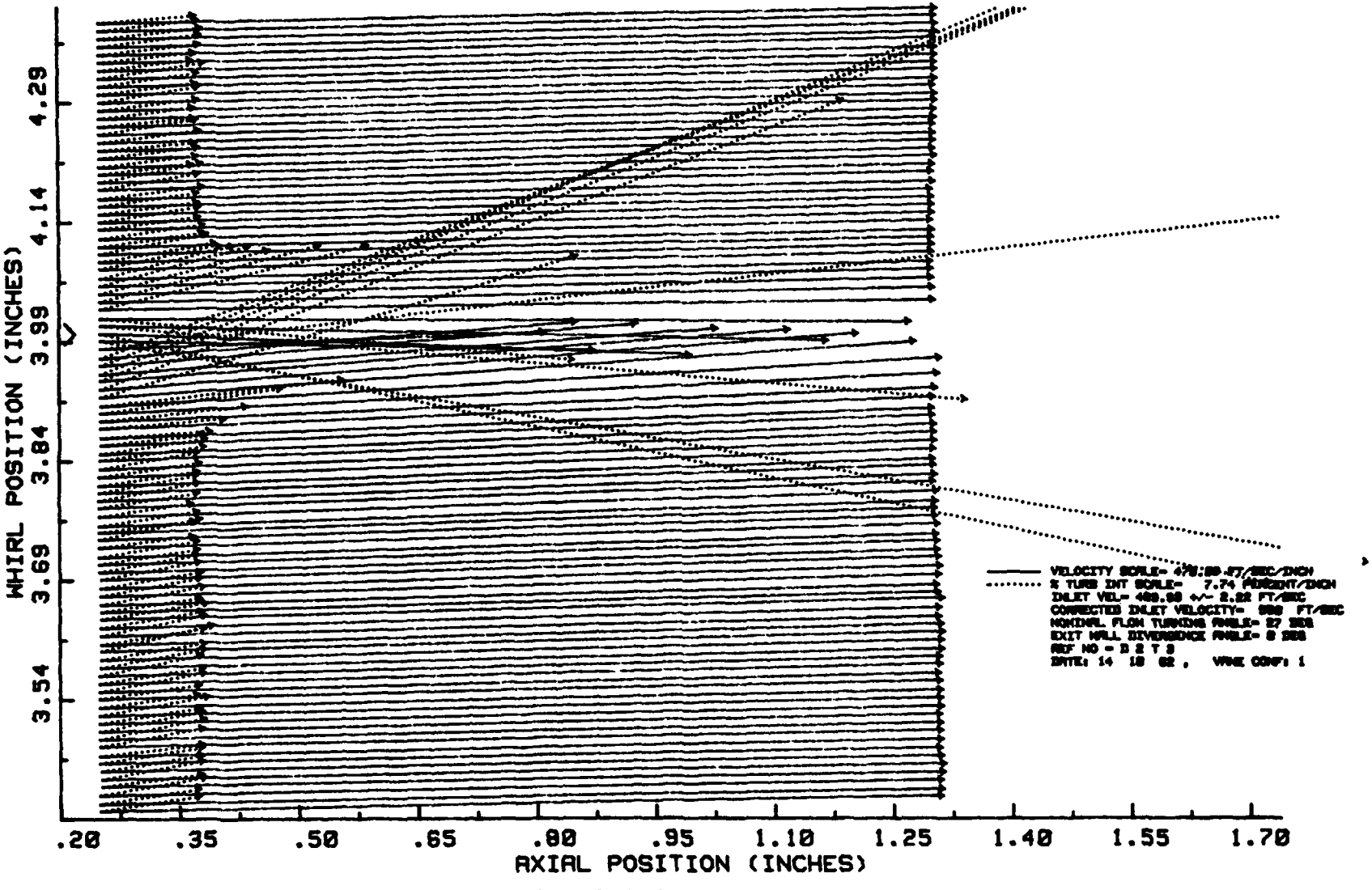

(a) .125 Chord Traverse

Figure 5. Smooth Vanes Velocity and Turbulence Intensity Profiles.

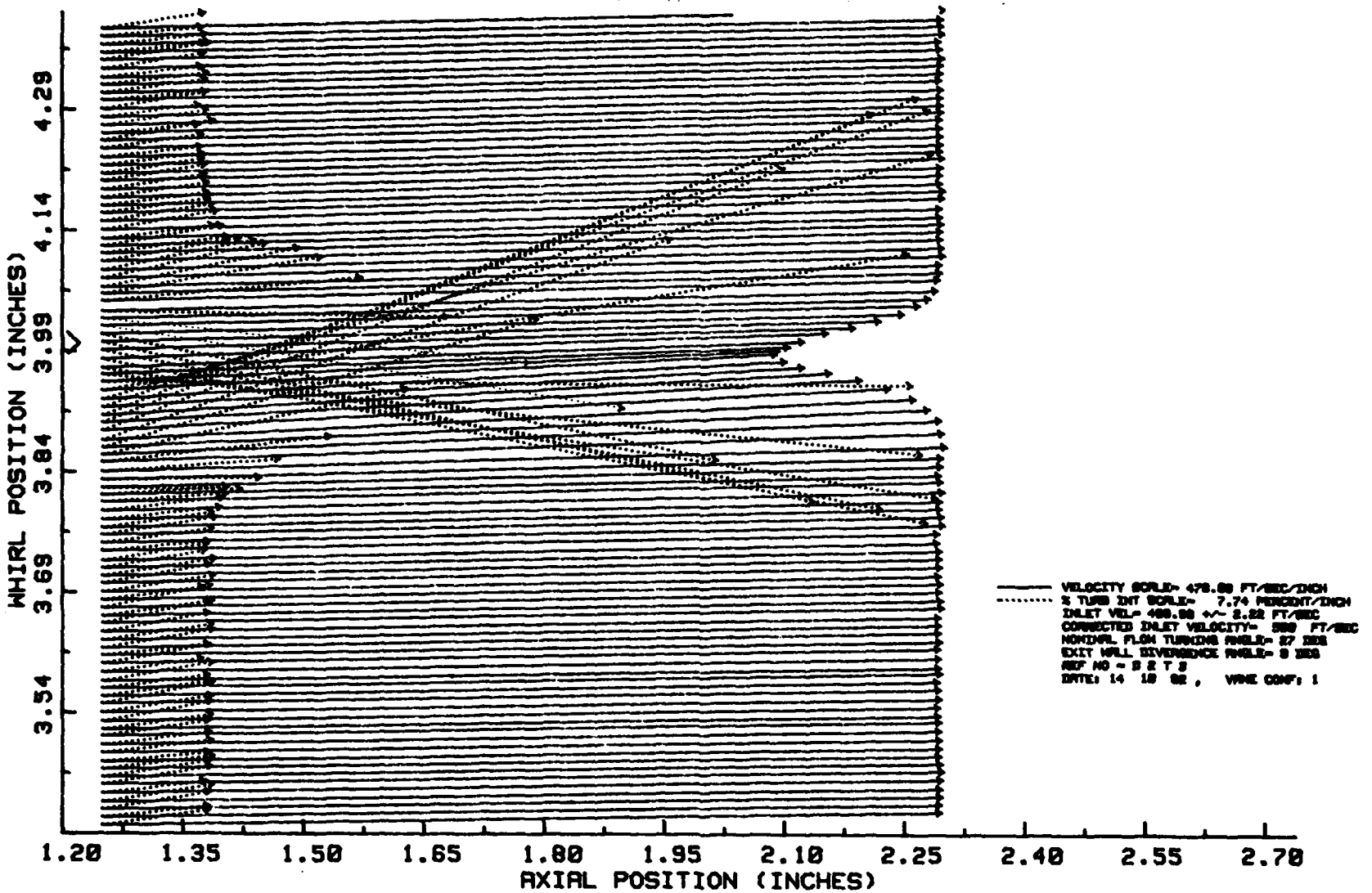

(b) .625 Chord Traverse

Figure 5.-Continued.

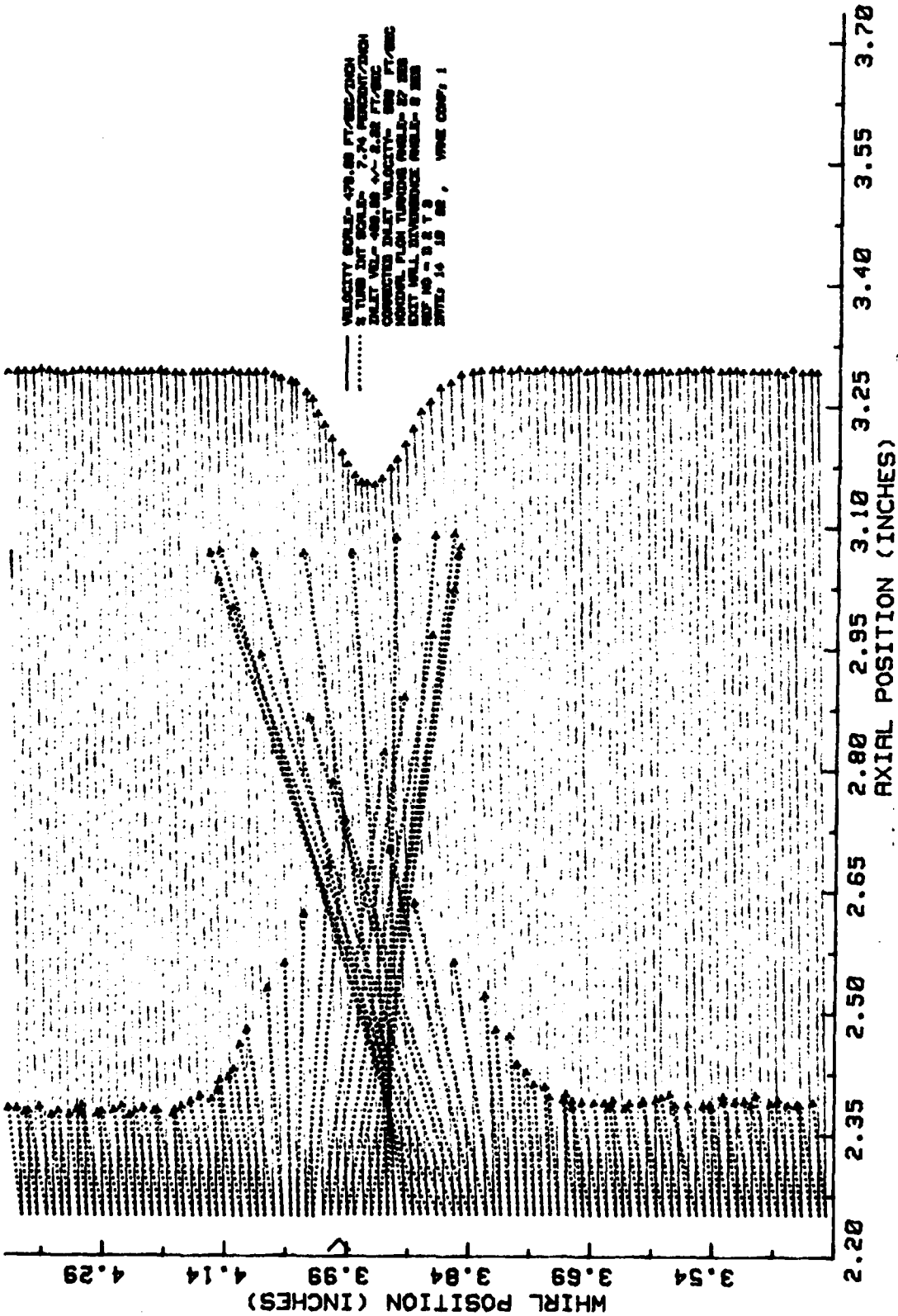

(c) 1.125 Chord Traverse

Figure 5.-Continued.

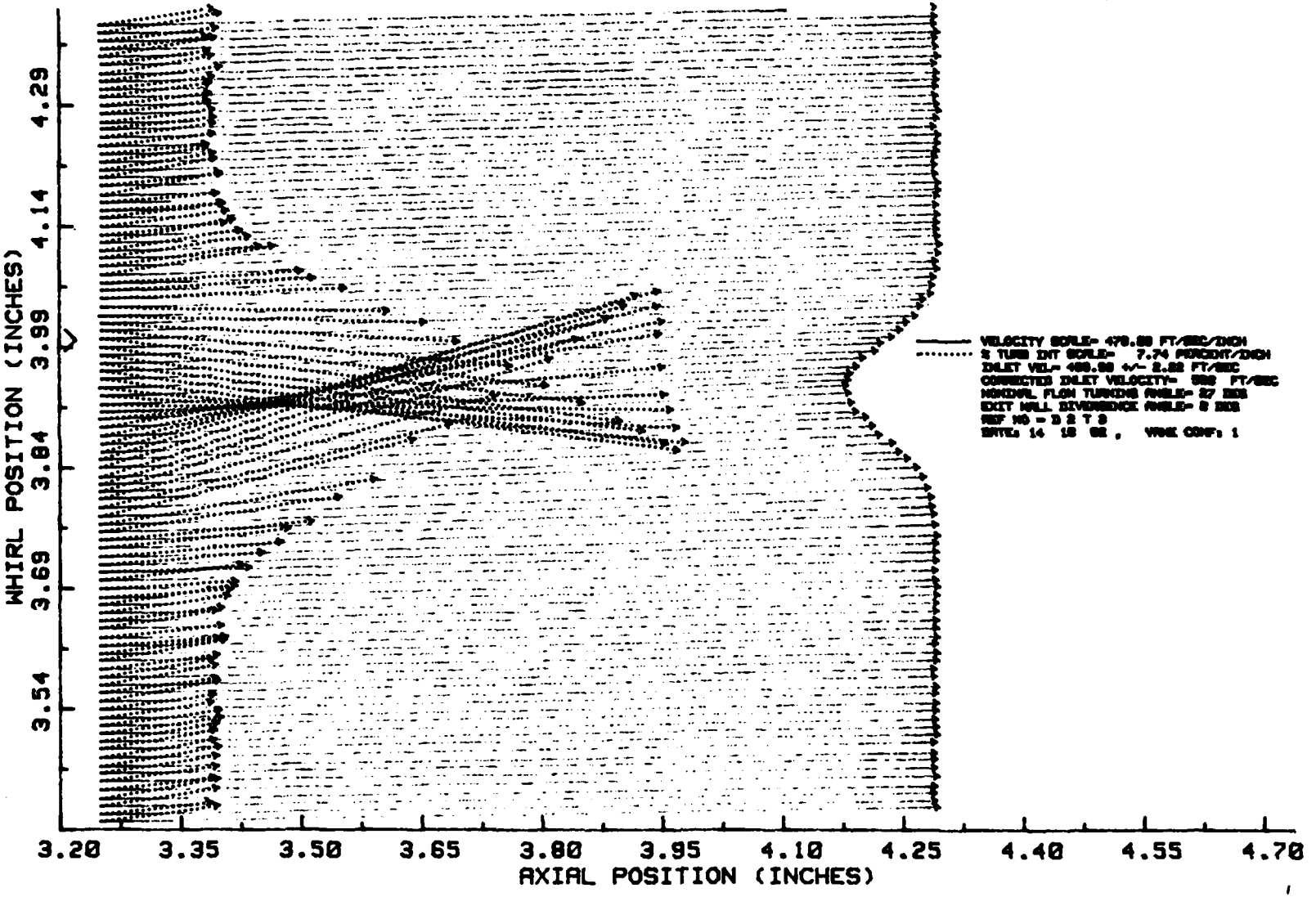

(d) 1.625 Chord Traverse

Figure 5.-Continued.

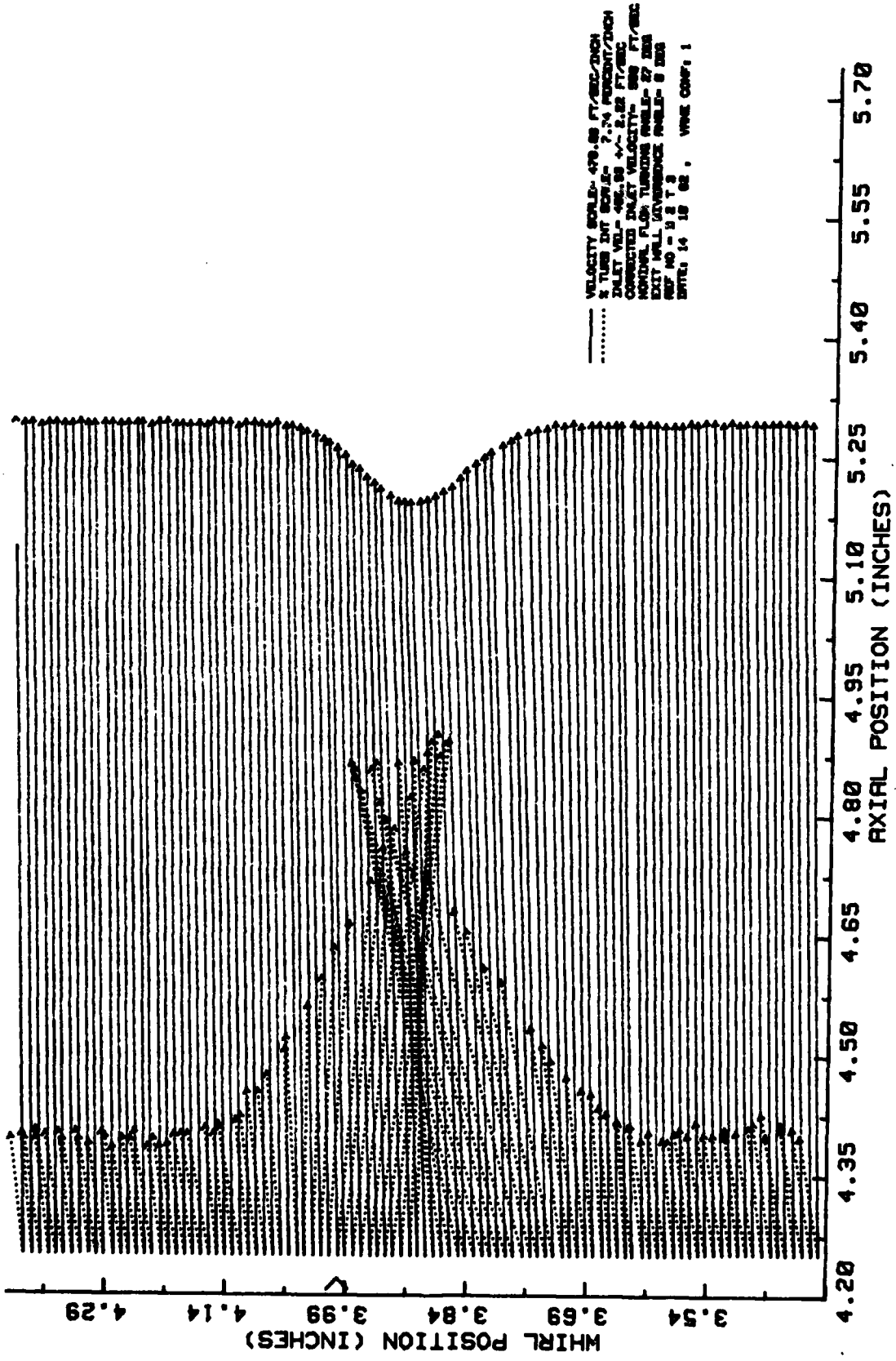

(e) 2.125 Chord Traverse

Figure 5.-Concluded.

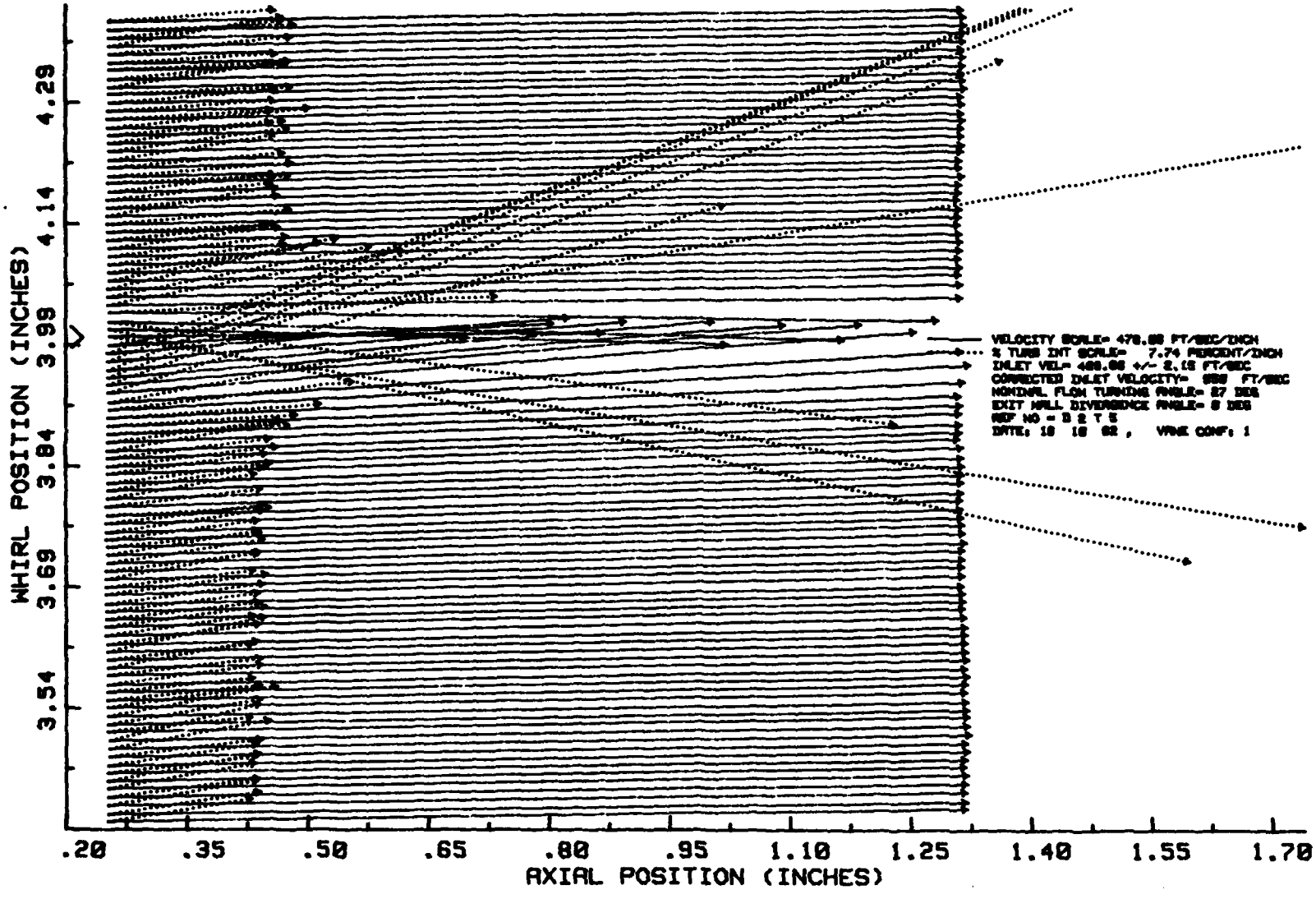

(a) .125 Chord Traverse

Figure 6. Rough Vanes Velocity and Turbulence Intensity Profiles.

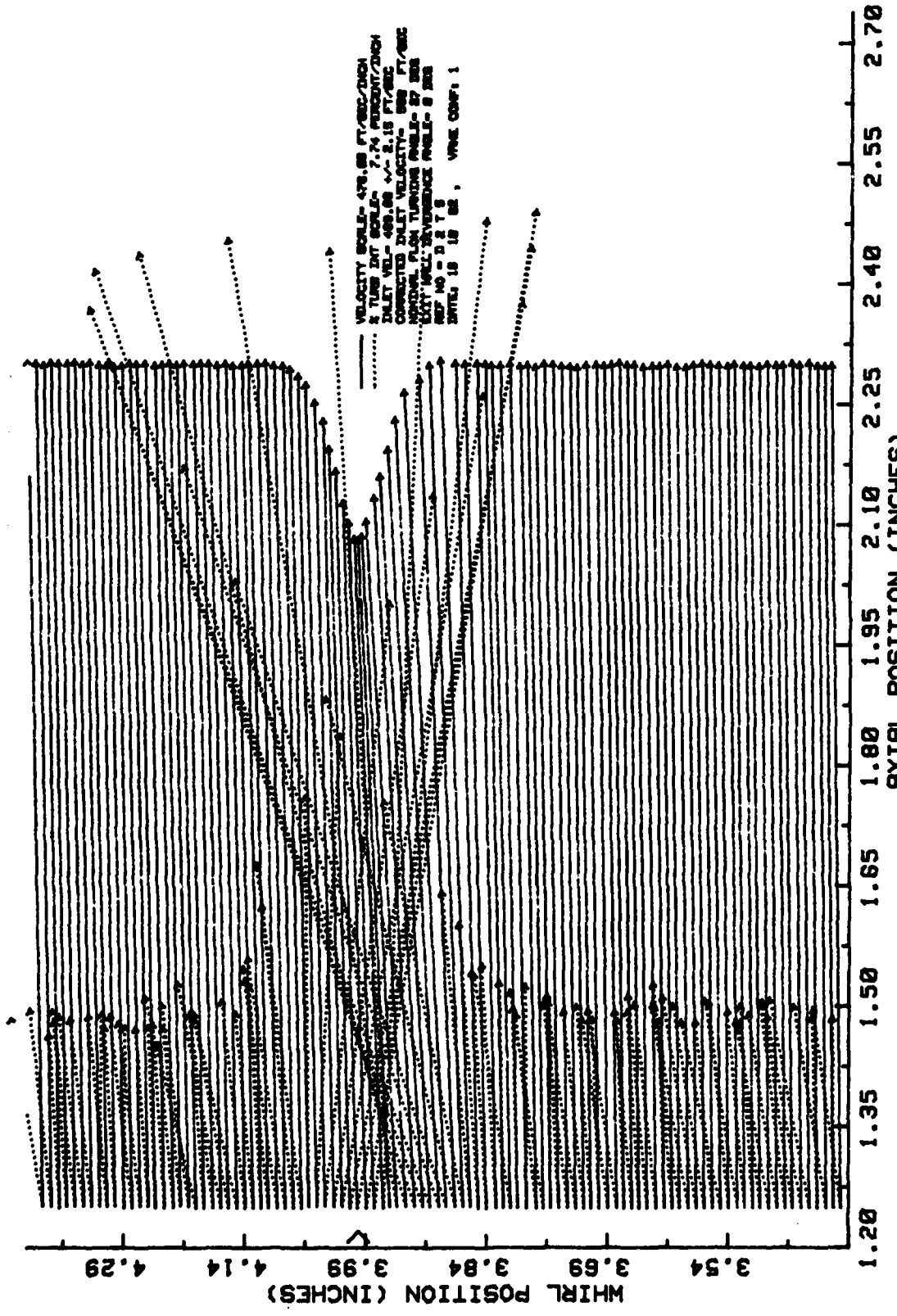

(b) .625 Chord Traverse

Figure 6.-Continued.

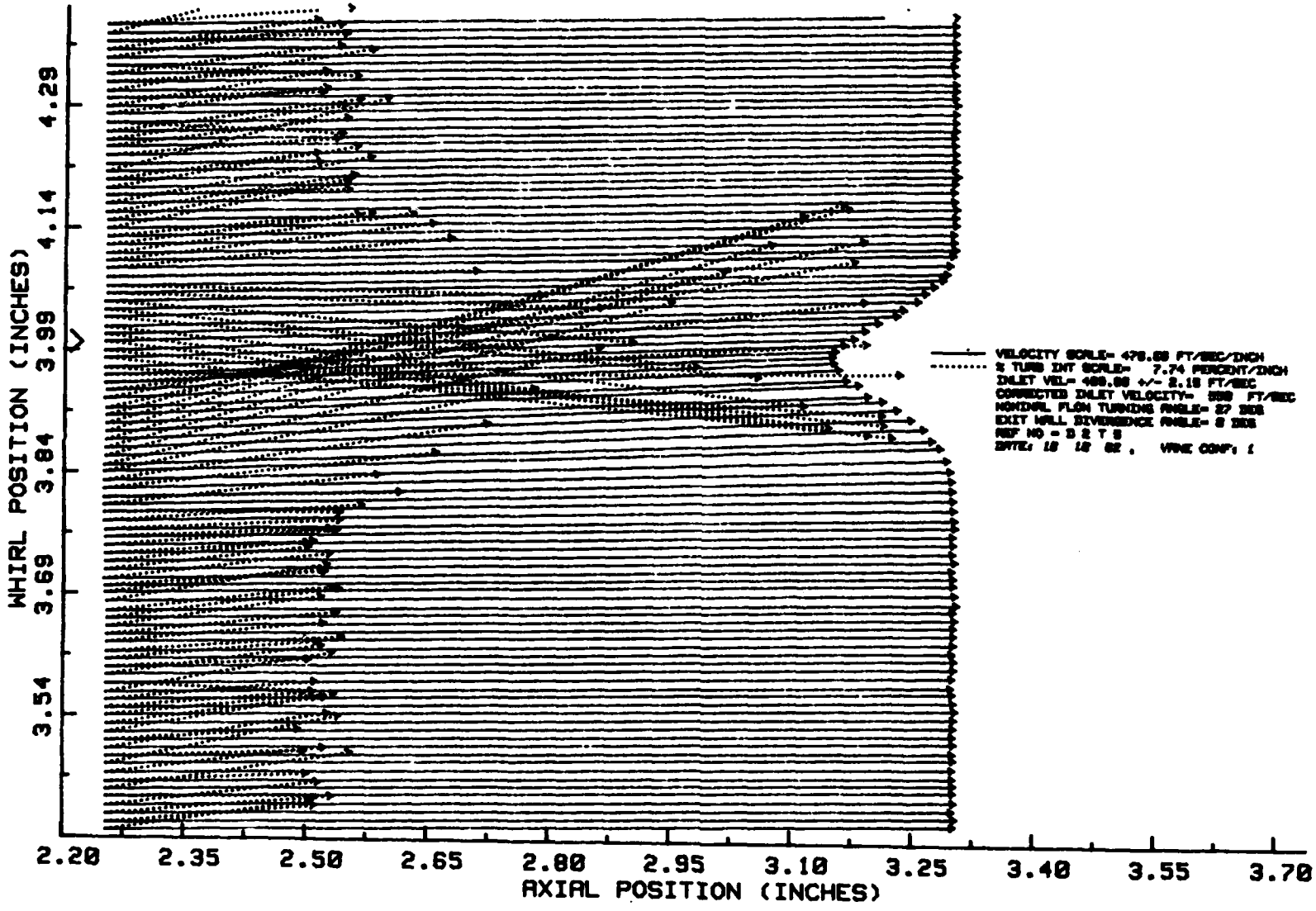

(c) 1.125 Chord Traverse

Figure 6.-Continued.

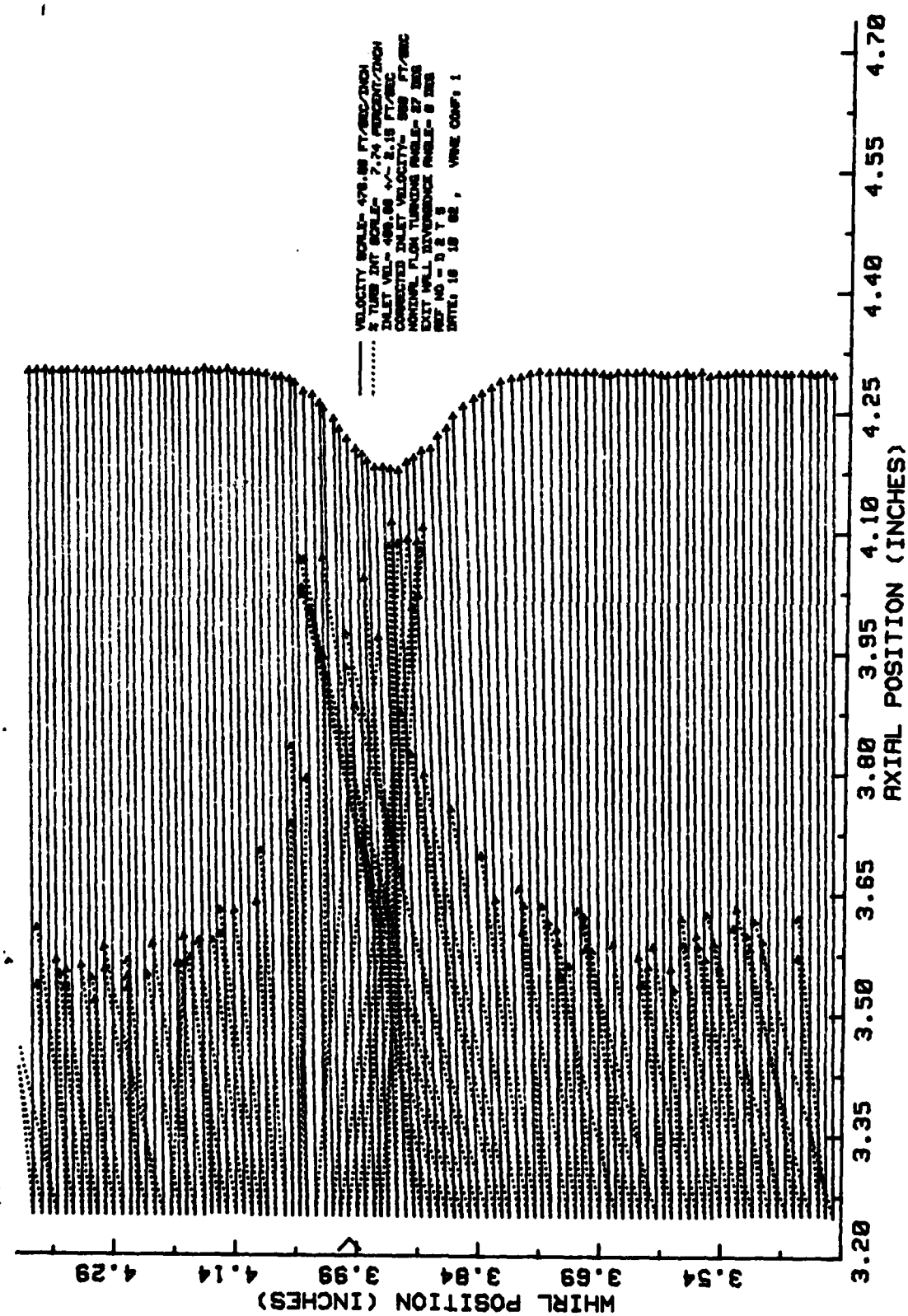

(d) 1.625 Chord Traverse

Figure 6.-Continued.

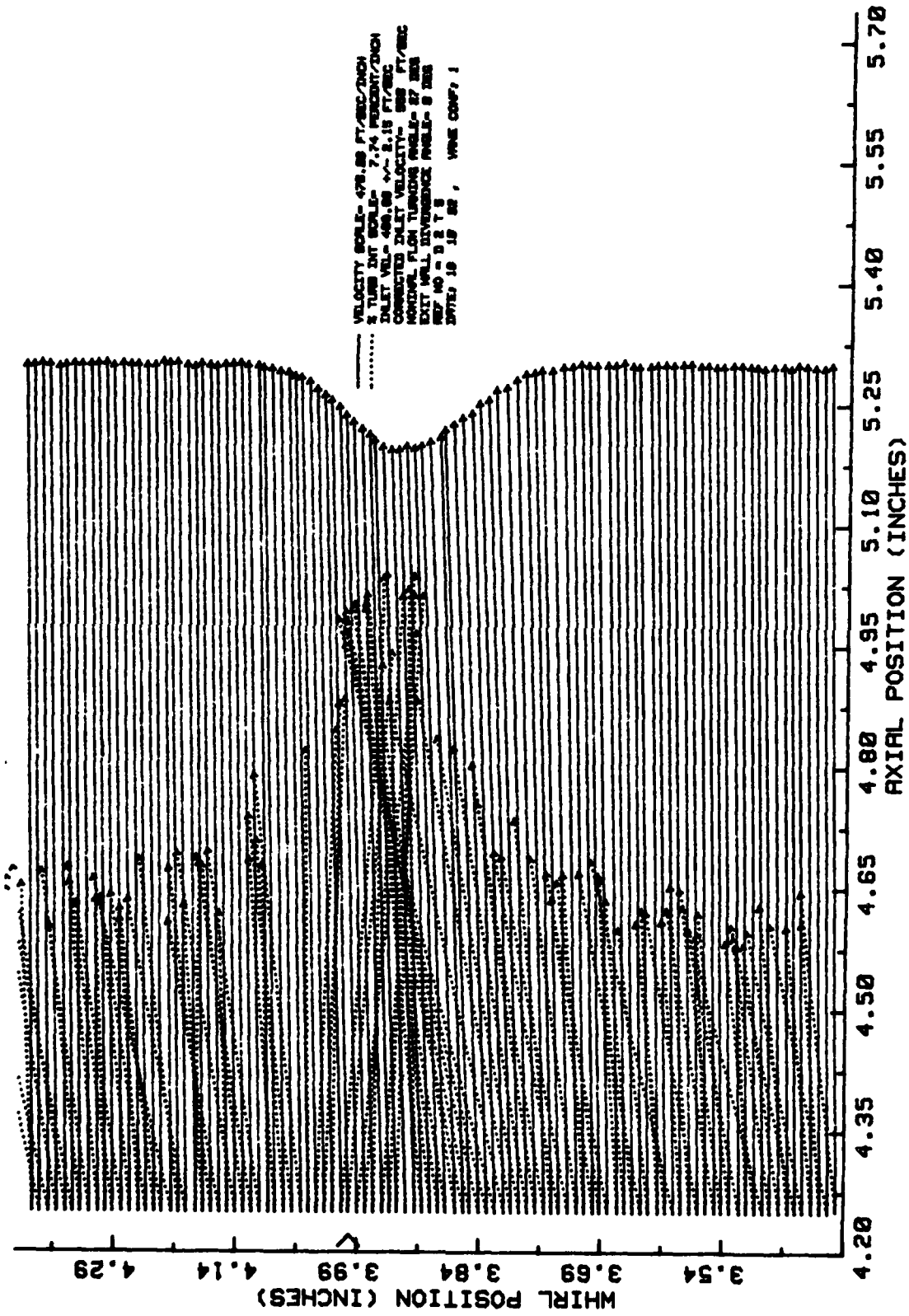

(e) 2.125 Chord Traverse

Figure 6.-Concluded.

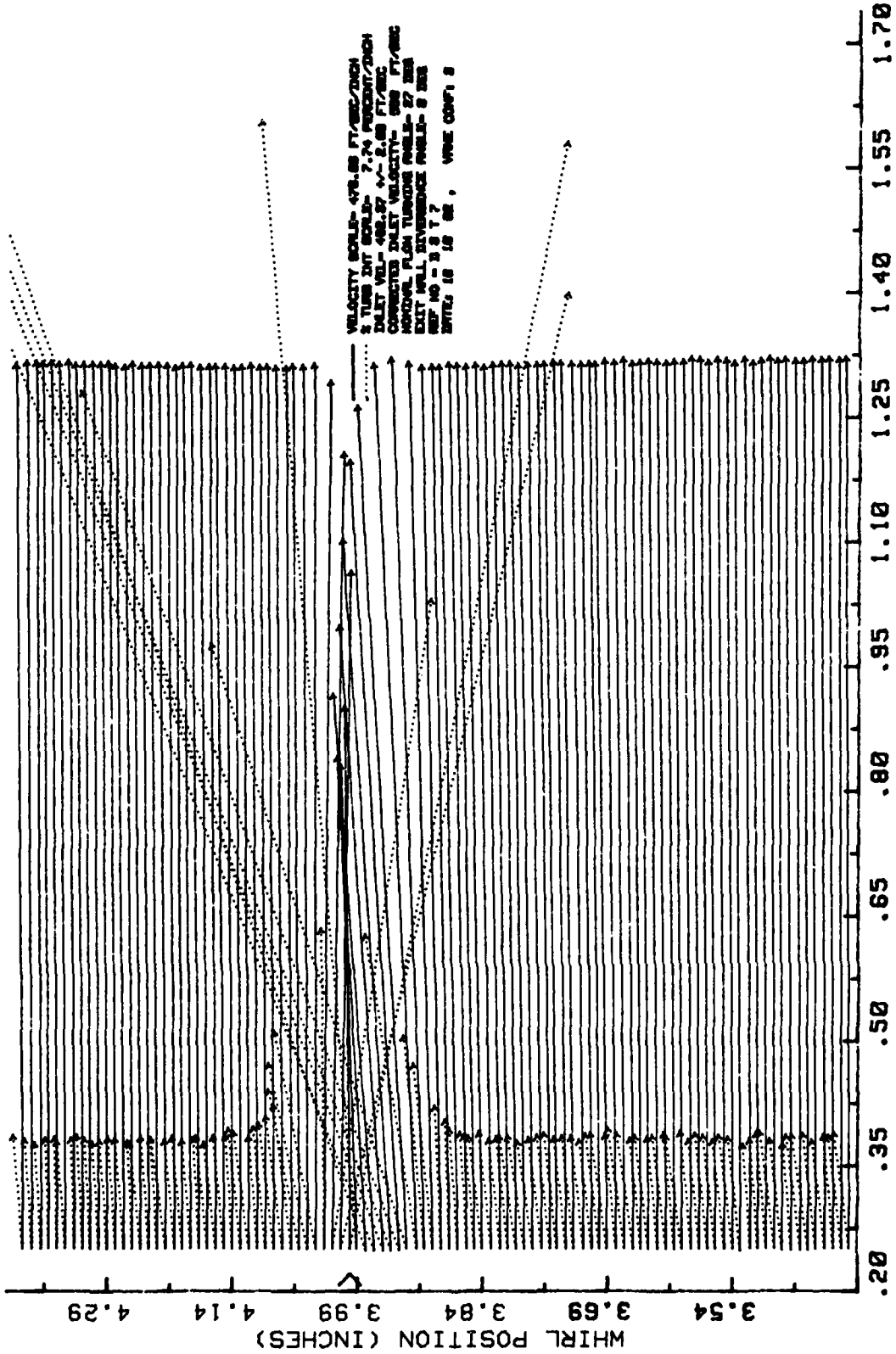

(a) .125 Chord Traverse

Figure 7. Rough Pressure Side Vanes Velocity and Turbulence Intensity Profiles.

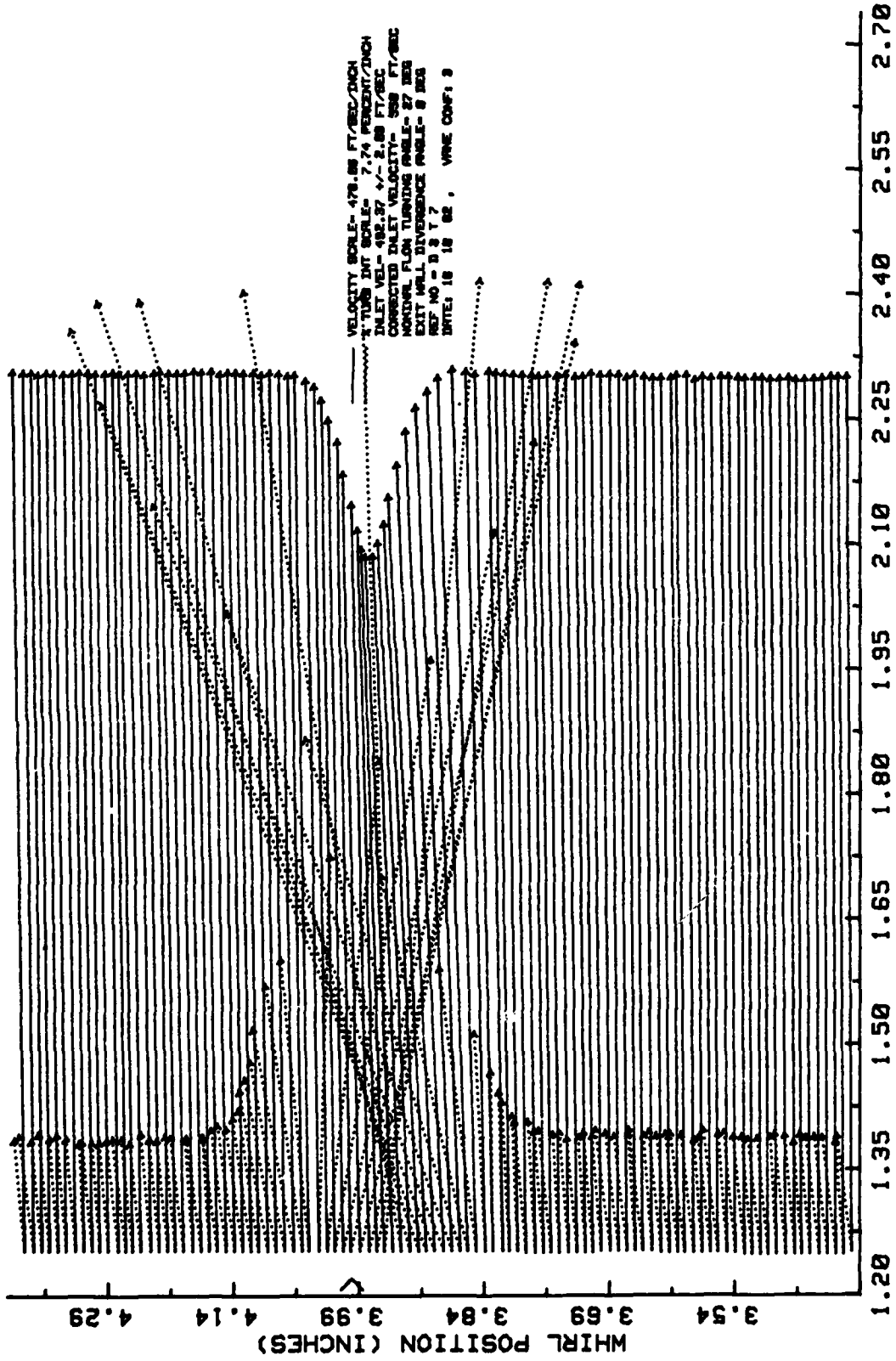

(b) .625 Chord Traverse

Figure 7.-Continued.

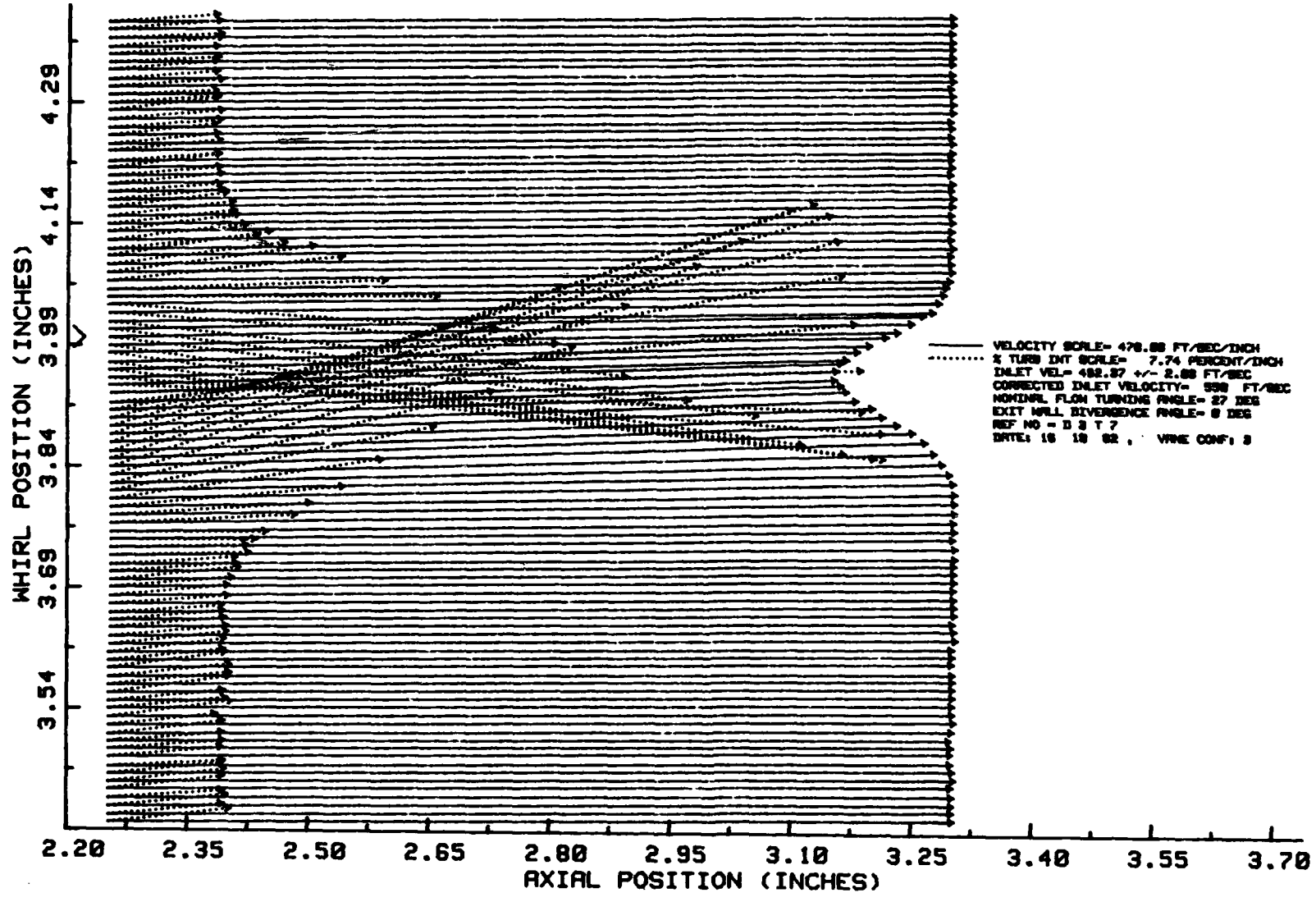

(c) 1.125 Chord Traverse

Figure 7.-Continued.

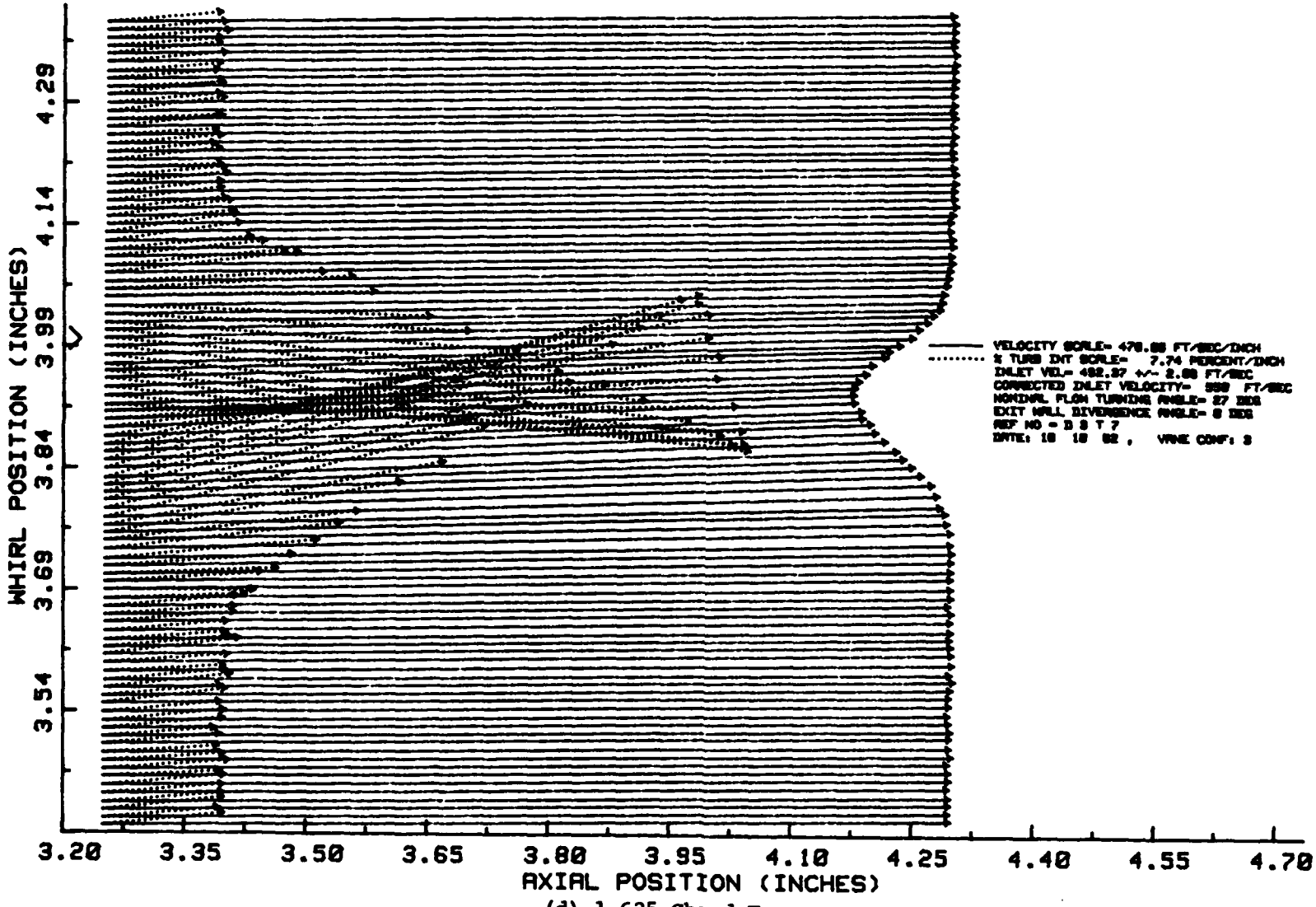

(d) 1.625 Chord Traverse

Figure 7.-Continued.

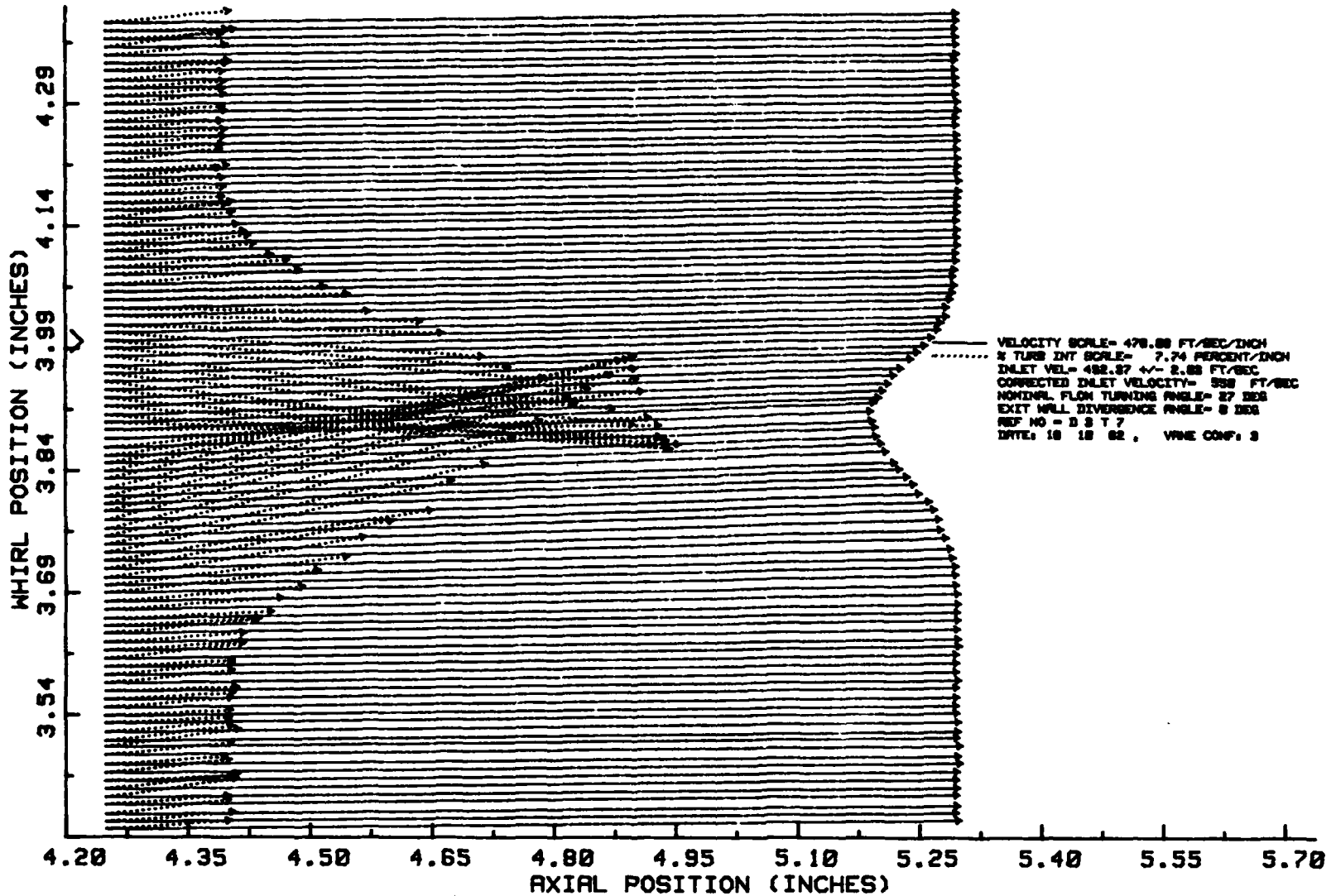

(e) 2.125 Chord Traverse

Figure 7.-Concluded.

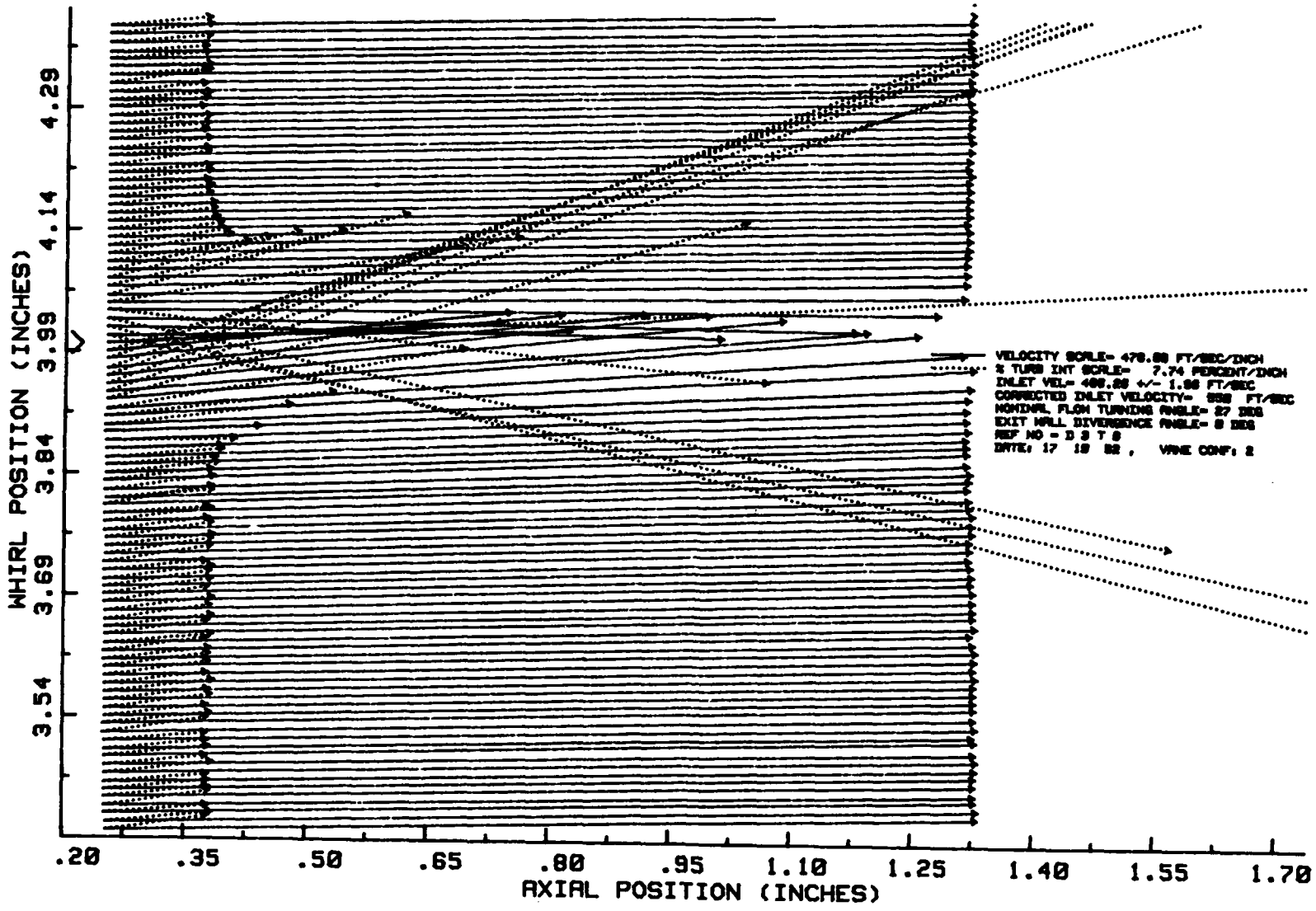

(a) .125 Chord Traverse

Figure 8. Rough Suction Side Vanes Velocity and Turbulence Intensity Profiles.

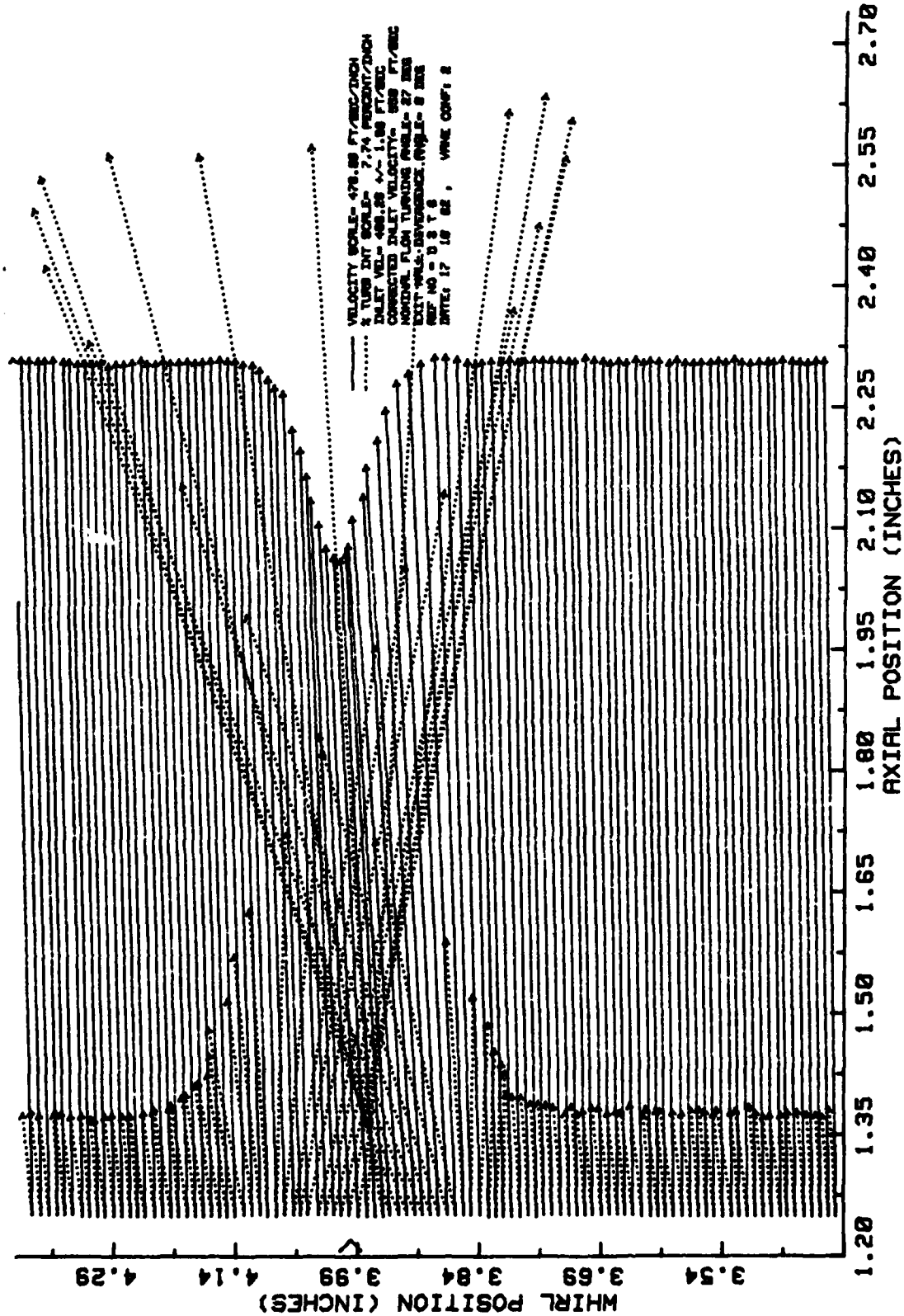

(b) .625 Chord Traverse

Figure 8.-Continued.

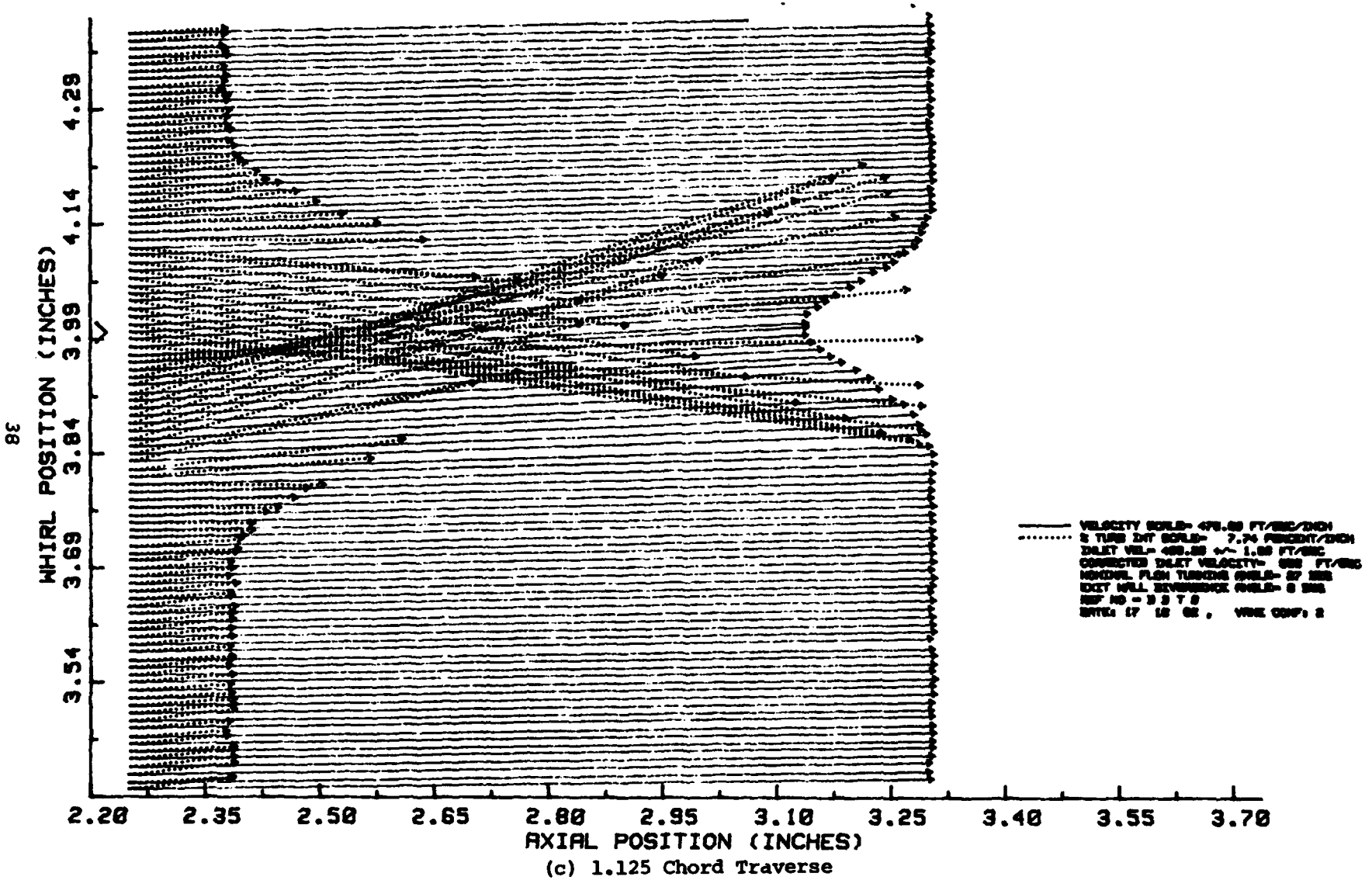

(c) 1.125 Chord Traverse

Figure 8.-Continued.

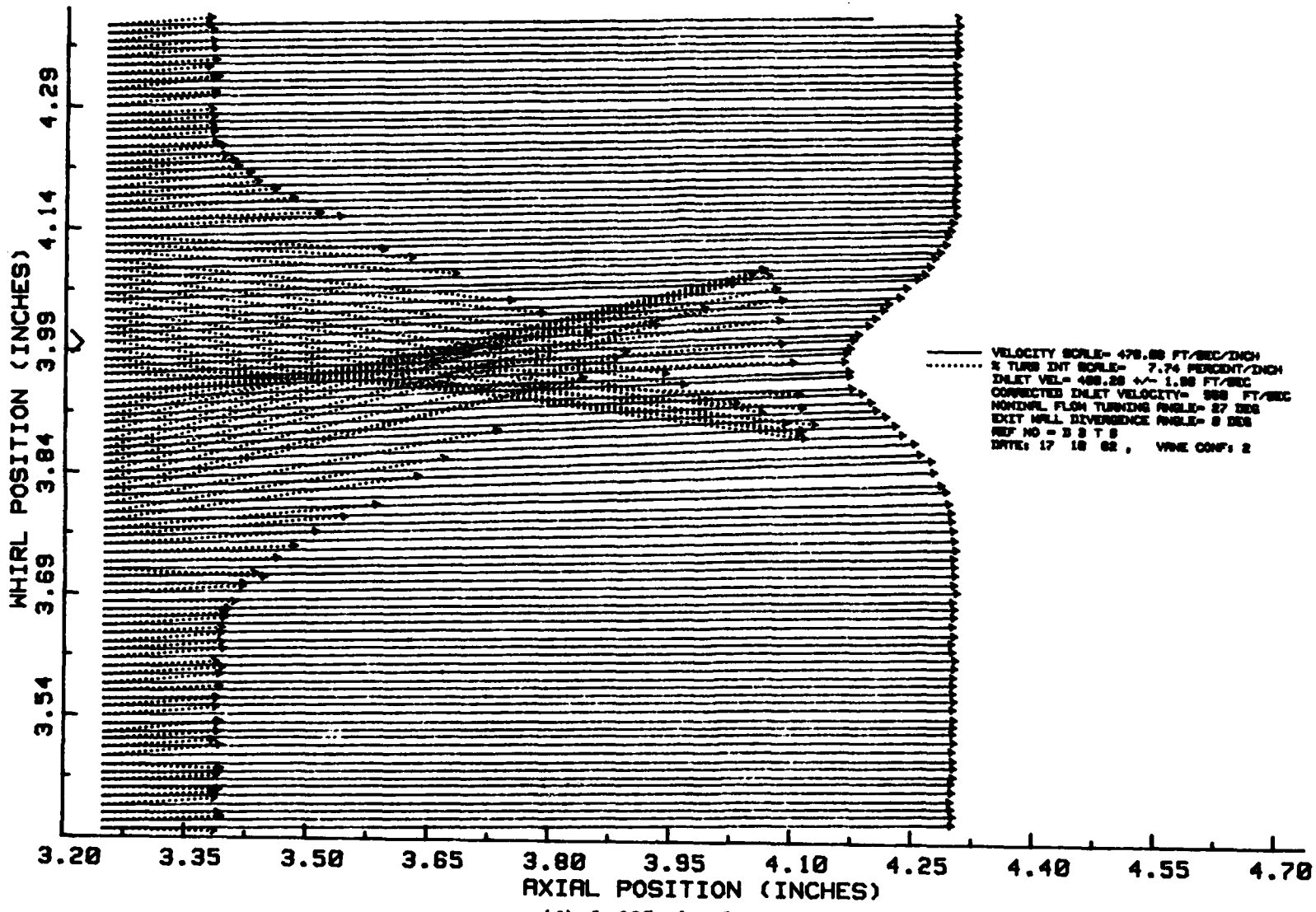

(d) 1.625 Chord Traverse

Figure 8.-Continued.

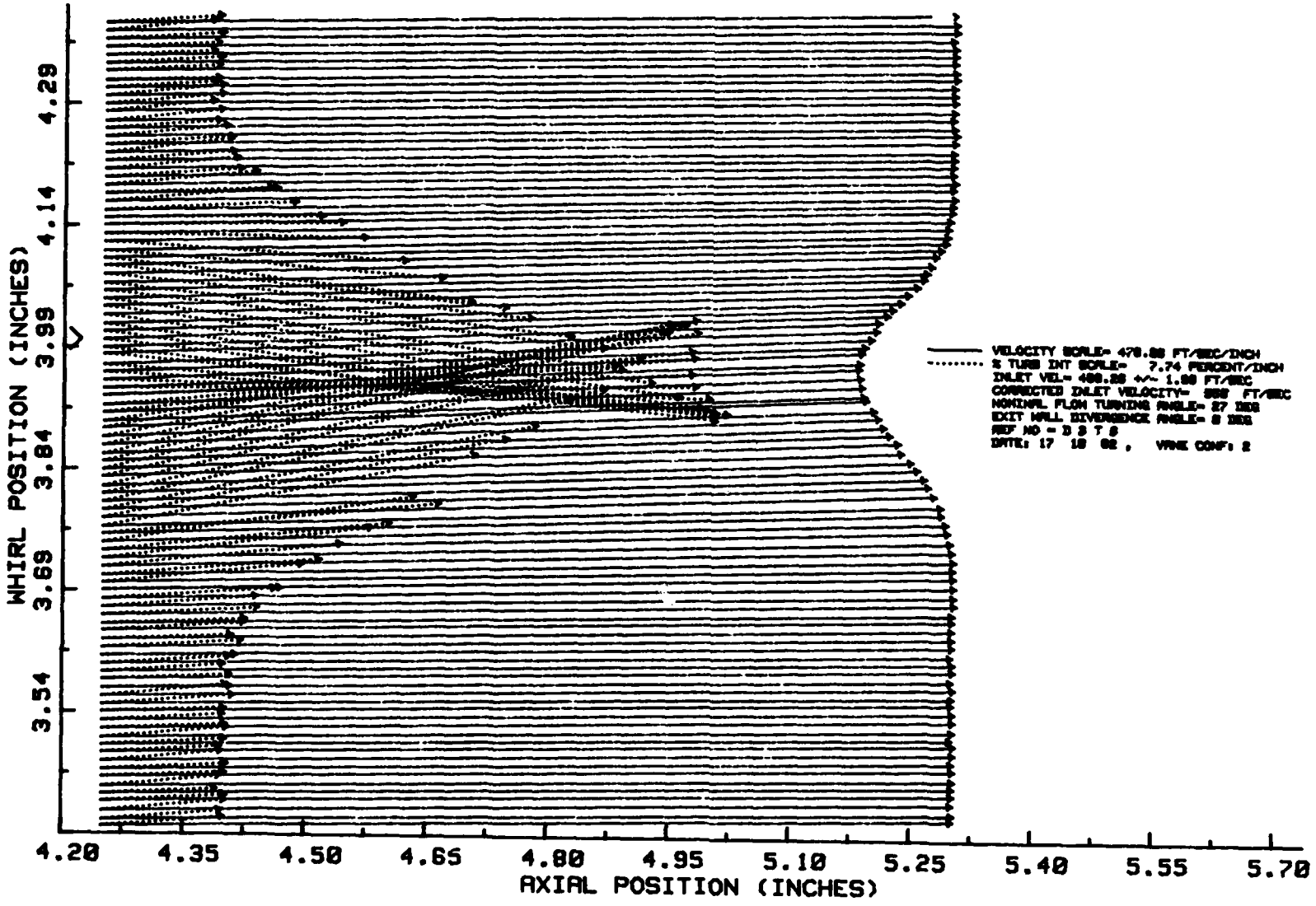

(e) 2.125 Chord Traverse

Figure 8.-Concluded.

Examination of the velocity and turbulnce intensity contours in Appendix C further substantiates the results discussed above. Each line on the plots is a contour of constant value which exists from plane to plane. These contours allow a visible evaluation of the trend of the data through comparison of the plots from the various testing configurations.

Comparison of the results of the rough surface vane test (Fig 6) with the smooth surface vane test (Fig 5) reveals differences in both the velocity and turbulence intensity profiles. Although the free stream velocity is the same for both tests, the velocity deficit for the rough blades is greater at the initial traverses, but becomes the same by the final traverse. The location of the velocity deficit for the rough blades is visibly shifted toward the pressure side of the vane. Additionally, the rough vane surface turbulence intensity is greater in both the free stream and the wake regions. A truncation of the turbulence intensity in the wake is evident on the suction side of the vane along with a broadening in the near wake wake region on both sides; considerably more so on the pressure side. A large increase in the free stream turbulence intensity is visible for the rough surface vanes.

Comparison of the rough pressure side surface vane test (Fig 7) with the results of the smooth surface vane test (Fig 5) reveals only slight effects on the flow. The velocity profile is nearly identical. A slightly higher free stream

turbulence intensity level (truncated on the suction side of the vane) is visible in the wake,and is accompanied by a small increase in the near wake turbulence intensity on the pressure side.

The effects of roughness on the suction side of the vane surface (Fig 8) are nearly as significant as roughness on both sides when compared to the smooth surface vane test (Fig 5). The free stream velocity is identical for both the smooth and rough configurations whereas the velocity decrement is both greater and shifted towards the pressure side for the suction side rough vanes at locations near the trailing edge. The free stream turbulence intensity is on the same order as the smooth vanes, but the wake values are greater on the suction side. The suction side also exibits a trunction of the turbulence intensity in the wake. The pressure side exibits a broadening of the turbulence intensity in the region near the wake.

Coefficient of Drag

The results of the calculation of the coefficient of drag are presented in Table II. The effect of roughness can be seen for all tests with rough surfaces however, the difference in the coefficient of drag is not great. This is a result of the high angle of attack which caused a separation of flow over the vanes. The separated condition tended to wash out the effect of the roughness. The largest coefficient of drag resulted from the vanes with roughness on the suction

side surface along with a smooth pressure side. The coefficient of drag for the vanes with roughness only on the pressure side was equal to the coefficient of drag for the vanes with roughness on both sides. The smooth surface vanes produced the lowest coefficient of drag. The probable effect of the roughness on the suction side was to energize the boundary layer near the leading edge of the airfoil thereby maintaining the flow in an attached state for a short additional distance along the vane. This was substantiated by the exibited truncation of turbulence intensity on the suction side of the vane accompanied by an increase in the magnitude of the upper wake values.

TABLE II

VANE SECTION DRAG COEFFICIENT

TEST CONFIGURATION	REYNOLDS NO/Ft (milion)	Cd
Smooth Vanes	3.8	.109
Rough Vanes	3.8	.110
Pressure Rough Vanes	3.9	.110
Suction Rough Vanes	3.9	.112

V. Conclusions and Recommendations

Conclusions

Surface roughness does affect the flow over outlet guide vanes at high Reynolds number and high turning angle. The effect manifests itself through an increase in the momentum deficit of the flow caused by the vanes. This increase in momentum deficit represents a decrease in the performance of the vanes as was indicated by the increased coefficient of drag for vanes with roughness on one or both sides. Additionally, surface roughness caused a change in the character of the flow which is evident from the visible shift of both the velocity and turbulence intensity profiles in the flow . The effects were most significant for the configuration of roughness on the suction side of the vane with the pressure side smooth. The high angle of attack caused separation of the flow over the vanes which reduced the ability to determine the effects of roughness.

Recommendations

A further investigation of the effects of rough compressor vanes should be performed with an experimental setup at a lower angle of attack in order to maintain attached flow over the vanes. This configuration would provide more visibility of the effects of the roughness. Test vanes should be made from metal using production manufacturing methods to better model actual vanes in use.

Bibliography

1. Hornbeck, Robert W. Numerical Methods, New York: Quantum Publishers, INC., 1975

2. Stiles, P.J. Roughness Effects in Axial Compressors-An Emperical Model-. Unpublished Report. Wright-Patterson AFB, Ohio: Wright Aernautical Laboratories, 1980.

3. Schaffler, A. "Experimental and Analytical Investigation of the Effects of Reynolds Number and Blade Surface roughness on Multistage Axial Flow Compressors," Journal of Engineering For Power, 102:5-13 (January 1980)

4. Taylor Hobson. Surtronic 3. Operating Instructions. Leicester, England: Rank Taylor Hobson, (undated).

5. Allison, Dennis M. Design and Evaluation of a Cascade Test Facility, Unpublished MS Thesis. Wright-Patterson AFB, Ohio: Air Force Institute of Technology, June 1982.

6. Rivir, Richard B., Wright Aeronautical Laboratories, (personal communication). Wright-Patterson AFB, Ohio, 1981.

7. Vonada, John A., Air Force Institute of Technology, (personal communication). Wright-Patterson AFB, Ohio, 1981.

8. Larsen, Soren E. and Busch, Niels E. "On the Humidity Sensitivity of Hot Wire Measurements".DISA Information No. 25: 4-5 (February 1980).

9. Pope, Alan. Wind-Tunnel Testing, New York; John Wiley and Sons, INC., 1954.

10. Bradshaw, P. An Introduction to Turbulence and Its Measurement, New York; Pergamon Press, INC., 1971.

Appendix A: Test Data Output

Example pages of the data acquisition and reduction system raw and reduced data are presented on the following pages. The pressure and temperature data are the basic data which are used to calculate the velocity data. The data presented is representative of that of all experimental tests performed.

FILE NAME D2T4 PRESSURE and TEMPERATURE DATA PAGE No. 12

DATA POINTS	Ps throat PSIG	Ps exit PSIG	Pt tank PSIG	P ambient PSIA	Pt ejector PSIG	Tt tank Deg F	T ambient Deg F
1	-.384	-.019	1.503	14.266	-.090	99.906	72.227
2	-.383	-.019	1.501	14.267	-.078	100.097	72.379
3	-.383	-.018	1.502	14.267	-.078	100.226	72.468
4	-.384	-.019	1.498	14.267	-.073	100.398	72.290
5	-.383	-.019	1.505	14.267	-.078	100.552	72.093
6	-.383	-.019	1.501	14.267	-.078	100.700	72.112
7	-.383	-.017	1.510	14.267	-.073	100.811	72.049
8	-.382	-.019	1.509	14.267	-.073	100.915	71.979
9	-.381	-.018	1.509	14.267	-.067	101.026	71.871
10	-.382	-.018	1.500	14.267	-.073	101.087	71.801
11	-.381	-.018	1.510	14.267	-.078	101.173	71.756
12	-.382	-.017	1.505	14.267	-.073	101.284	71.604
13	-.381	-.017	1.503	14.266	-.084	101.327	71.515
14	-.379	-.017	1.504	14.267	-.067	101.456	71.425
15	-.381	-.017	1.508	14.267	-.067	101.604	71.355
16	-.379	-.017	1.509	14.267	-.073	101.672	71.381
17	-.381	-.016	1.508	14.267	-.073	101.819	71.266
18	-.381	-.016	1.503	14.267	-.073	101.862	71.266
19	-.381	-.017	1.495	14.267	-.073	101.991	71.132
20	-.380	-.017	1.503	14.267	-.073	102.077	70.999
21	-.382	-.018	1.506	14.268	-.050	102.206	71.043
22	-.381	-.017	1.503	14.267	-.050	102.206	71.043
23	-.381	-.017	1.505	14.267	-.050	102.292	71.088
24	-.382	-.017	1.499	14.267	-.056	102.335	70.910
25	-.381	-.017	1.501	14.267	-.056	102.421	70.731
26	-.380	-.017	1.506	14.267	-.056	102.507	70.687
27	-.381	-.017	1.507	14.257	-.056	102.550	70.687
28	-.381	-.016	1.503	14.269	-.050	102.679	70.598
29	-.379	-.017	1.501	14.263	-.050	102.722	70.731
30	-.378	-.016	1.508	14.257	-.056	102.764	70.865
31	-.380	-.015	1.506	14.267	-.050	102.850	70.820
32	-.381	-.017	1.503	14.267	-.056	102.850	70.553
33	-.380	-.017	1.498	14.267	-.050	102.936	70.687
34	-.381	-.018	1.504	14.263	-.062	102.979	70.642
35	-.380	-.017	1.506	14.267	-.062	103.022	70.776
36	-.380	-.017	1.500	14.268	-.067	103.108	70.553
37	-.380	-.017	1.508	14.268	-.067	103.230	70.591
38	-.381	-.017	1.504	14.269	-.062	103.237	70.508
39	-.380	-.016	1.498	14.267	-.067	103.255	70.616
40	-.382	-.016	1.507	14.268	-.062	103.280	70.598
41	-.391	-.016	1.503	14.267	-.057	103.262	70.534
42	-.380	-.016	1.503	14.268	-.052	103.366	70.687
43	-.381	-.017	1.506	14.267	-.062	103.409	70.865
44	-.380	-.016	1.496	14.267	-.073	103.409	70.954
45	-.381	-.016	1.505	14.267	-.067	103.434	71.025
46	-.381	-.016	1.504	14.267	-.073	103.519	71.114
47	-.381	-.017	1.502	14.268	-.052	103.623	71.222
48	-.380	-.015	1.498	14.267	-.067	103.623	71.266
49	-.380	-.016	1.497	14.267	-.067	103.665	71.311
50	-.381	-.017	1.504	14.267	-.067	103.648	71.381

FILE NAME 02T4 VELOCITY DATA PAGE No. 2

DATA POINT	X cord. INCHES	Y cord. INCHES	Ux mean ft/sec	Turbulence Int.X,%	Ux rms ft/sec	Uy mean ft/sec	Turbulence Int.Y,%	Uy rms ft/sec	Vel inlet ft/sec	Vel exit ft/sec	Um&Vexit % Error
1	.248	3.400	455.256	1.137	5.177	7.602	.111	.507	490.583	438.738	3.8
2	.248	3.409	455.032	1.179	5.363	7.252	.170	.775	490.284	438.360	3.8
3	.248	3.420	455.157	1.124	5.114	7.493	.160	.730	490.386	438.411	3.8
4	.248	3.430	454.284	1.196	5.435	8.128	.211	.958	490.105	438.015	3.7
5	.248	3.440	454.224	1.170	5.313	7.157	.146	.662	490.913	439.062	3.5
6	.248	3.450	455.447	1.165	5.304	7.791	.176	.801	490.611	438.642	3.8
7	.248	3.460	454.487	1.151	5.229	8.108	.131	.595	491.630	439.629	3.4
8	.248	3.469	454.709	1.079	4.903	7.903	.094	.428	491.536	439.799	3.4
9	.248	3.481	455.066	1.109	5.046	8.288	.108	.492	491.336	439.665	3.5
10	.248	3.490	453.865	1.194	5.418	8.481	.175	.794	490.403	438.431	3.5
11	.248	3.500	455.032	1.157	5.267	8.025	.159	.723	491.516	439.813	3.5
12	.248	3.510	454.547	1.118	5.084	8.647	.106	.483	491.079	439.110	3.5
13	.248	3.520	454.094	1.193	5.419	8.845	.223	1.012	490.692	438.816	3.5
14	.248	3.530	454.167	1.246	5.657	8.591	.209	.950	490.693	439.119	3.4
15	.248	3.541	453.726	1.190	5.398	8.610	.179	.814	491.516	439.644	3.2
16	.248	3.550	453.912	1.123	5.099	8.586	.138	.624	491.395	439.813	3.2
17	.248	3.560	454.475	1.111	5.050	8.744	.139	.633	491.618	439.662	3.4
18	.248	3.569	454.178	1.164	5.288	9.824	.161	.731	491.084	438.981	3.5
19	.248	3.581	454.259	1.119	5.081	9.814	.121	.550	490.095	437.994	3.7
20	.248	3.590	454.189	1.241	5.639	9.543	.166	.754	491.014	439.184	3.4
21	.248	3.600	453.401	1.138	5.159	10.068	.095	.431	491.688	439.683	3.1
22	.248	3.610	453.971	1.158	5.259	10.083	.178	.810	491.096	439.251	3.4
23	.248	3.620	453.363	1.134	5.140	10.245	.161	.728	491.476	439.517	3.2
24	.248	3.630	453.545	1.150	5.216	10.352	.139	.632	490.822	438.701	3.4
25	.248	3.641	453.074	1.128	5.111	10.323	.150	.682	491.031	439.053	3.2
26	.248	3.649	453.681	1.152	5.225	11.014	.194	.879	491.547	439.690	3.2
27	.248	3.660	453.321	1.246	5.651	10.996	.246	1.113	491.892	439.850	3.1
28	.248	3.670	453.062	1.169	5.296	11.503	.232	1.053	491.264	439.160	3.2
29	.248	3.680	453.066	1.200	5.436	11.532	.169	.764	490.746	439.107	3.2
30	.248	3.691	452.832	1.128	5.109	11.566	.187	.845	491.609	439.921	2.9
31	.248	3.700	452.817	1.162	5.260	11.259	.182	.823	491.649	439.483	3.0
32	.248	3.709	452.942	1.162	5.264	11.686	.235	1.064	491.371	439.342	3.1
33	.248	3.720	452.235	1.118	5.054	12.185	.158	.714	490.813	438.883	3.0
34	.248	3.730	452.359	1.171	5.299	12.422	.200	.904	491.556	439.743	2.9
35	.248	3.740	451.733	1.088	4.915	13.111	.127	.575	491.758	439.813	2.7
36	.248	3.750	452.108	1.144	5.172	12.742	.176	.794	491.040	438.998	3.0
37	.248	3.760	452.161	1.153	5.211	12.741	.154	.694	491.982	440.222	2.7
38	.248	3.769	452.507	1.136	5.139	13.171	.142	.641	491.701	439.783	2.9
39	.248	3.780	451.965	1.125	5.085	13.024	.104	.470	490.922	438.798	3.0
40	.248	3.790	451.218	1.116	5.034	13.944	.159	.719	492.129	439.920	2.6
41	.248	3.800	450.873	1.132	5.103	13.776	.114	.515	491.624	439.388	2.6
42	.248	3.810	451.670	1.131	5.110	13.434	.130	.587	491.472	439.509	2.8
43	.248	3.819	450.356	1.127	5.075	13.838	.127	.573	492.101	440.060	2.3
44	.248	3.831	451.390	1.173	5.293	14.077	.101	.455	490.767	438.529	2.9
45	.248	3.840	450.978	1.103	4.975	14.419	.120	.541	491.934	439.817	2.5
46	.248	3.850	450.728	1.141	5.142	14.625	.122	.550	491.845	439.683	2.5
47	.248	3.859	451.416	1.168	5.271	14.763	.133	.602	491.722	439.677	2.7
48	.248	3.869	450.994	1.266	5.711	15.465	.044	.197	491.124	438.774	2.8
49	.248	3.881	449.959	1.411	6.347	16.240	.072	.323	490.968	438.845	2.5
50	.248	3.891	452.218	1.754	7.932	17.800	.184	.833	491.886	439.844	2.8

Appendix B: Velocity and Turbulence Profiles

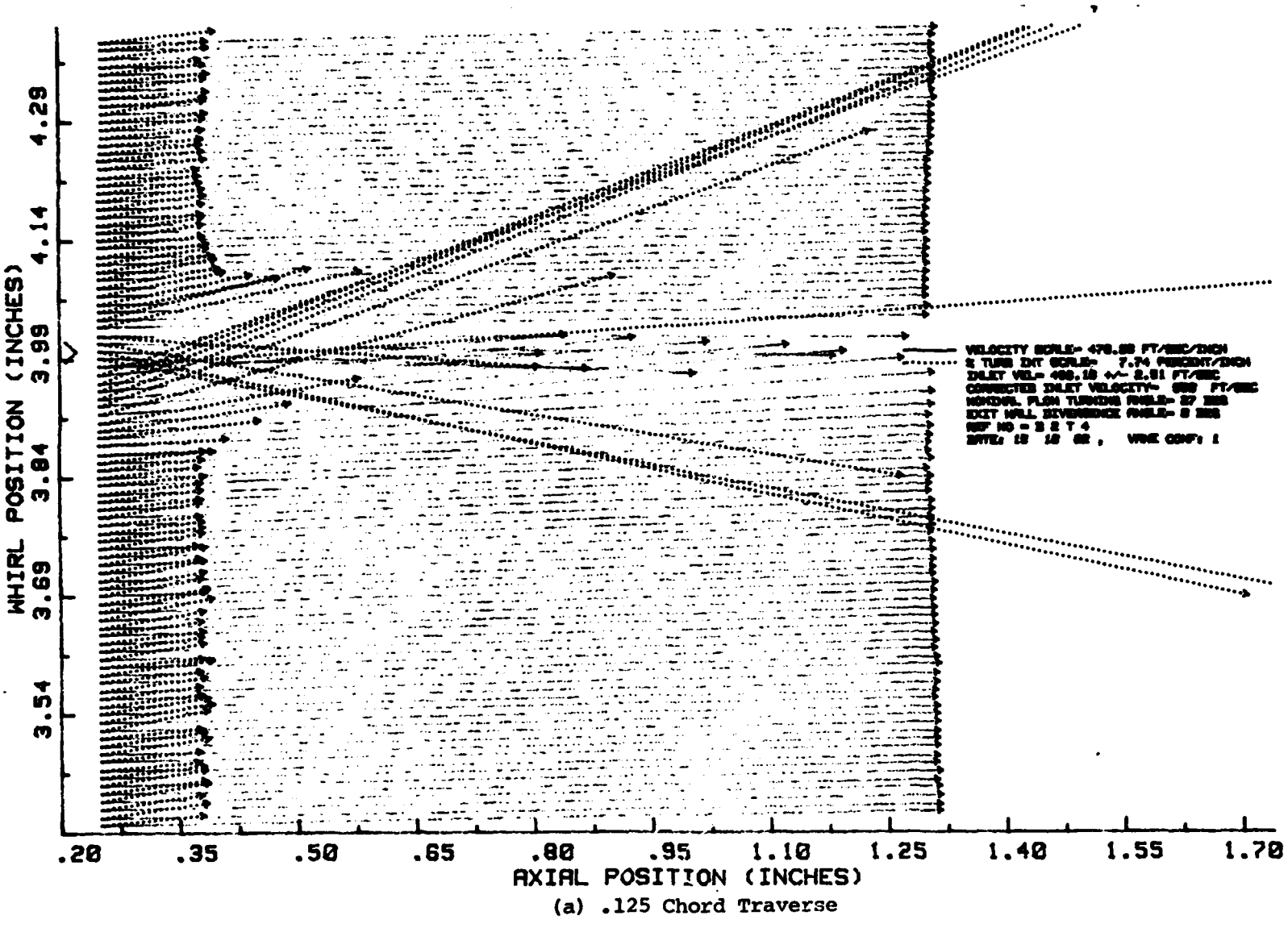

(a) .125 Chord Traverse

Figure 9. Smooth Vanes Test No 2 Velocity and Turbulence Intensity Profiles.

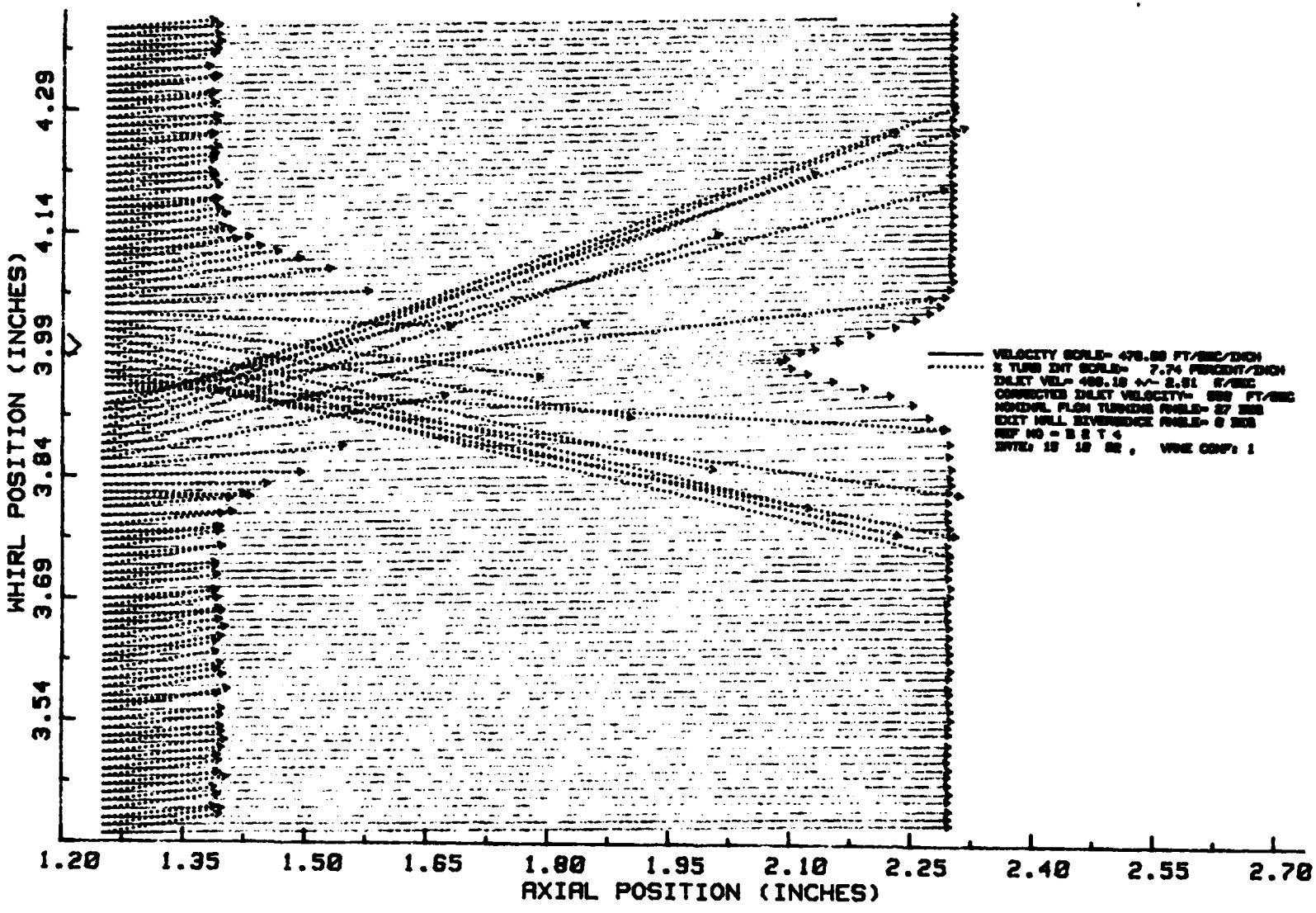

(b) .625 Chord Traverse

Figure 9.-Continued.

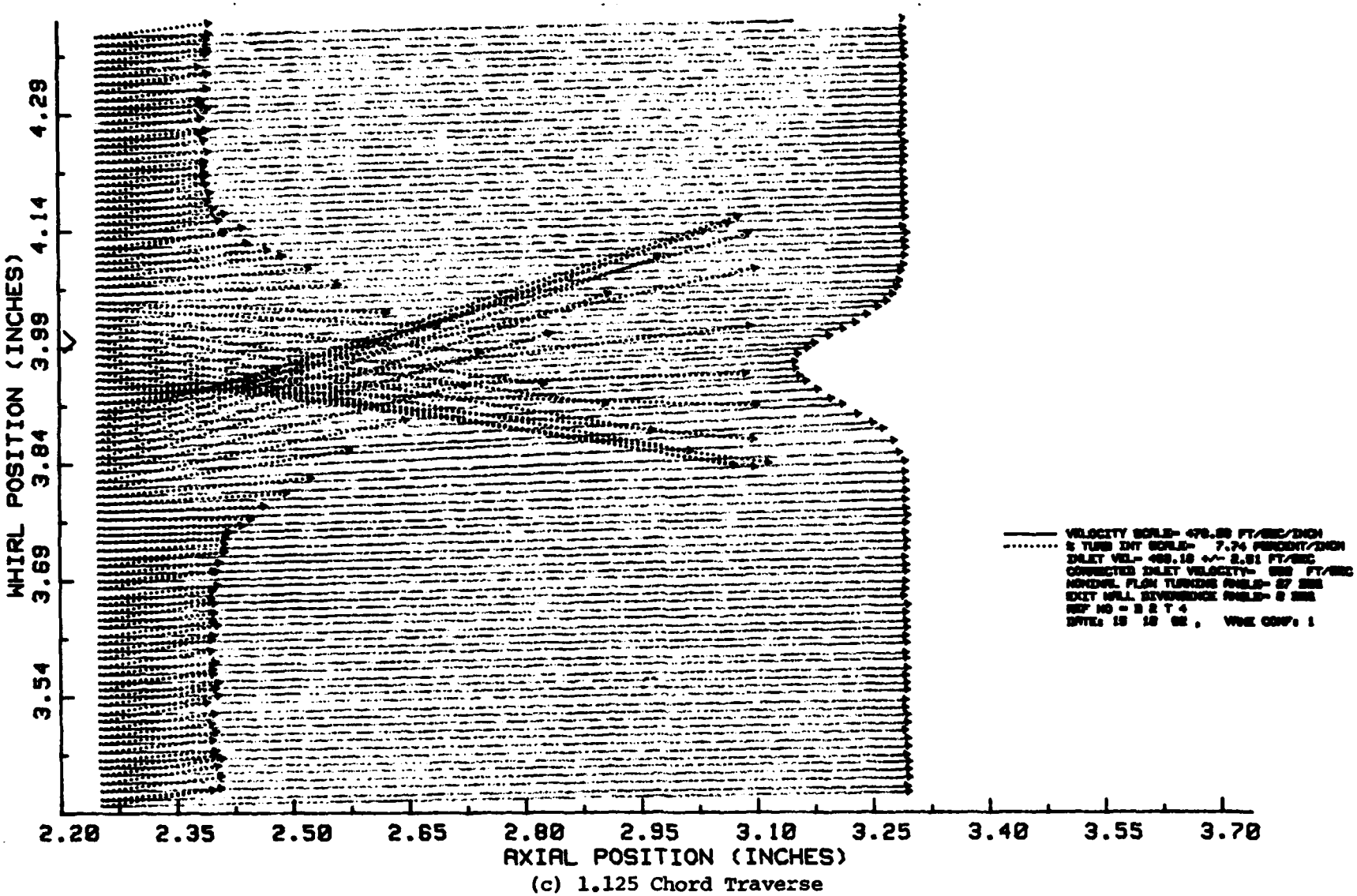

(c) 1.125 Chord Traverse

Figure 9.-Continued.

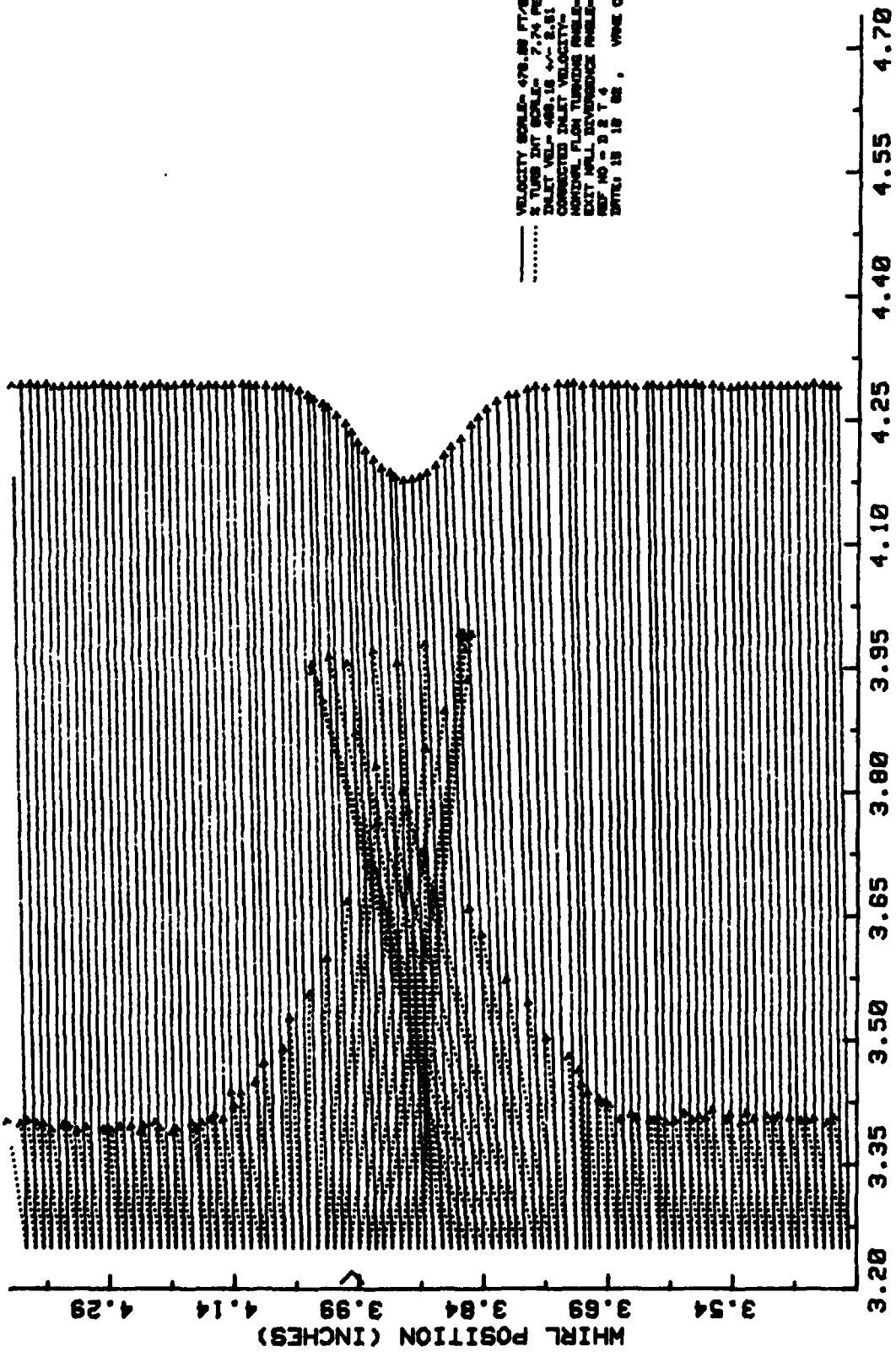

(d) 1.625 Chord Traverse

Figure 9.-Continued.

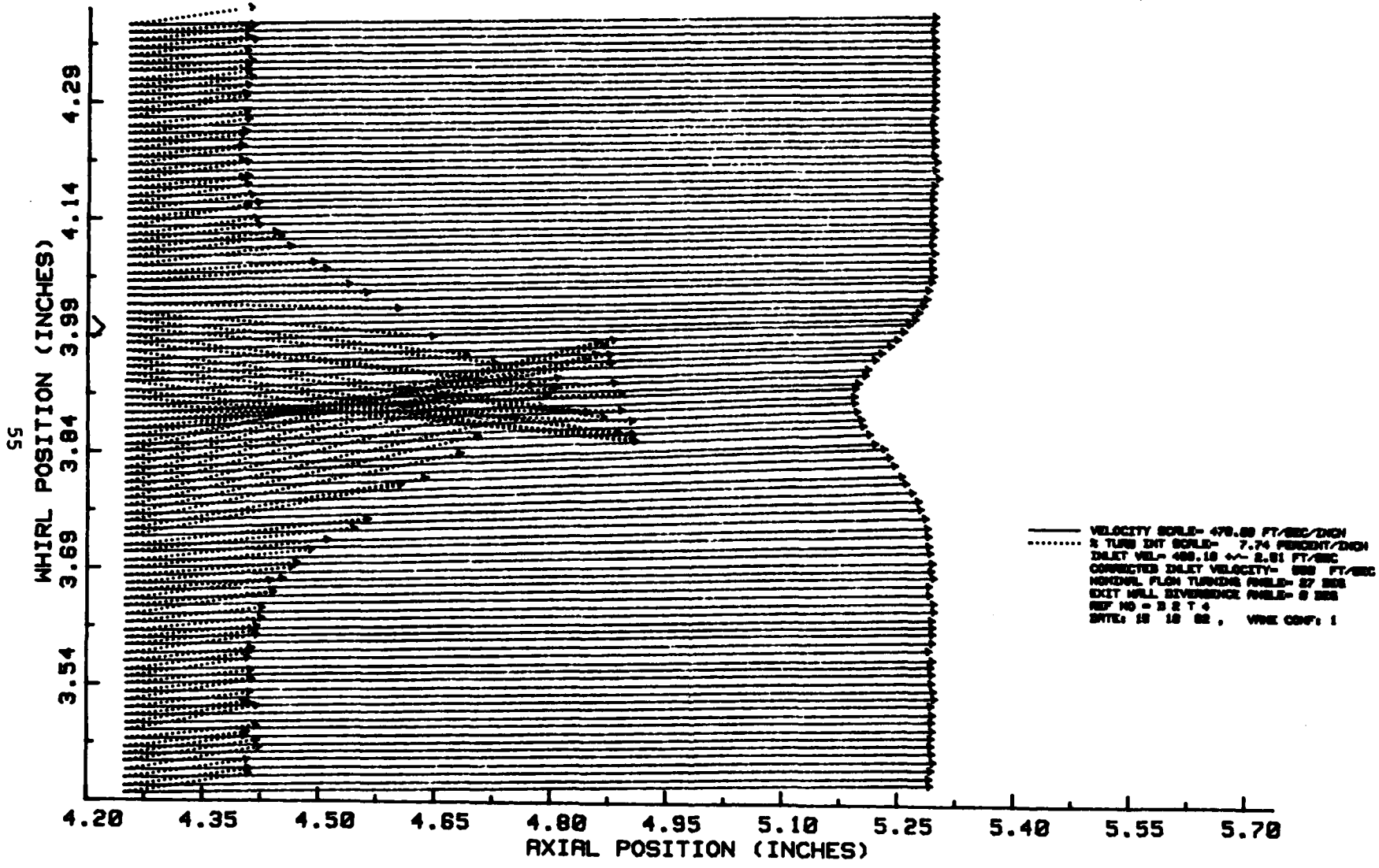

(e) 2.125 Chord Traverse

Figure 9.-Concluded.

Appendix C: Velocity and Turbulence Contours

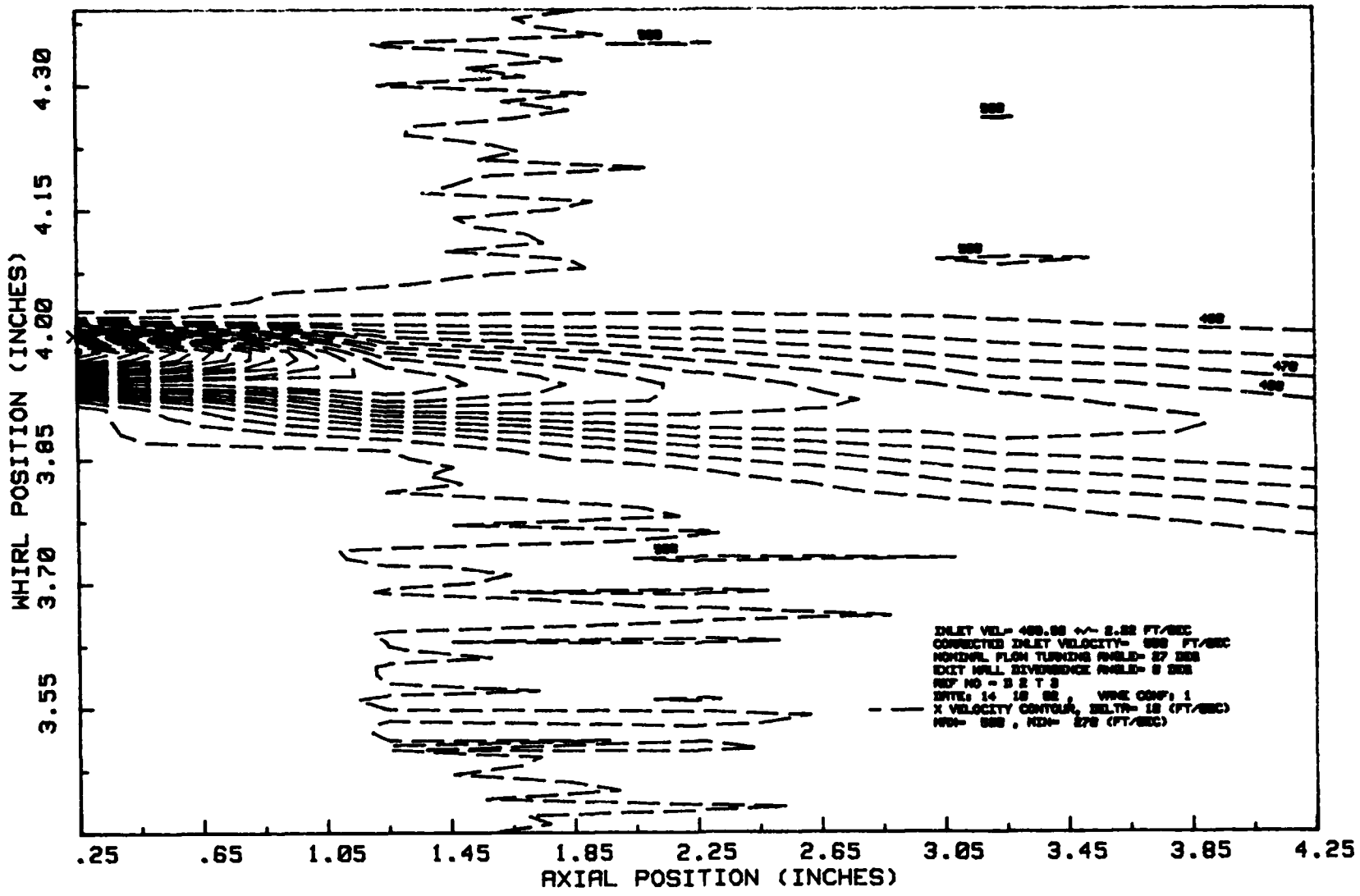

(a) X Velocity Contours

Figure 10. Smooth Vanes Velocity and Turbulence Intensity Contours.

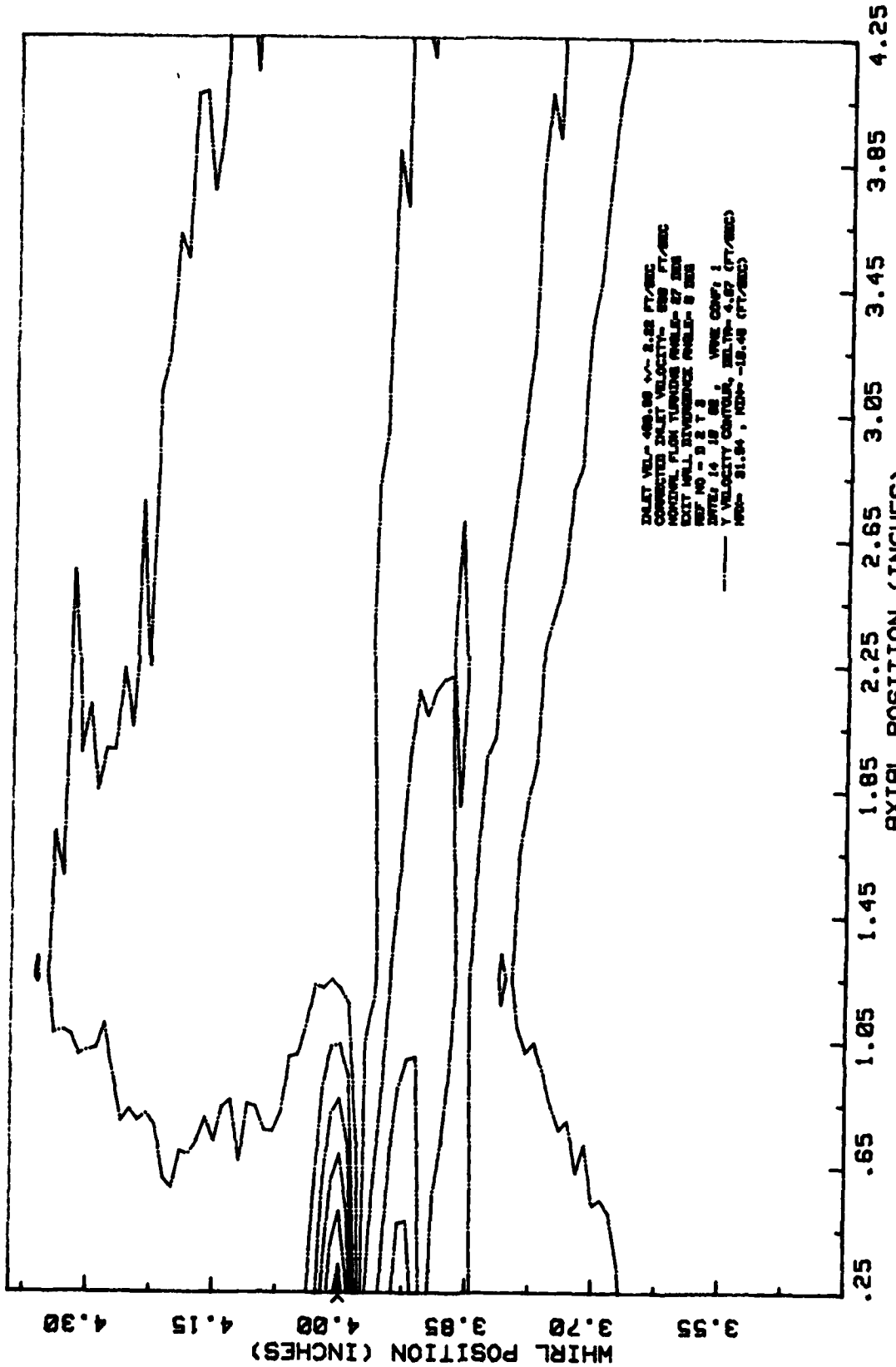

(b) Y Velocity Contours

Figure 10.-Continued.

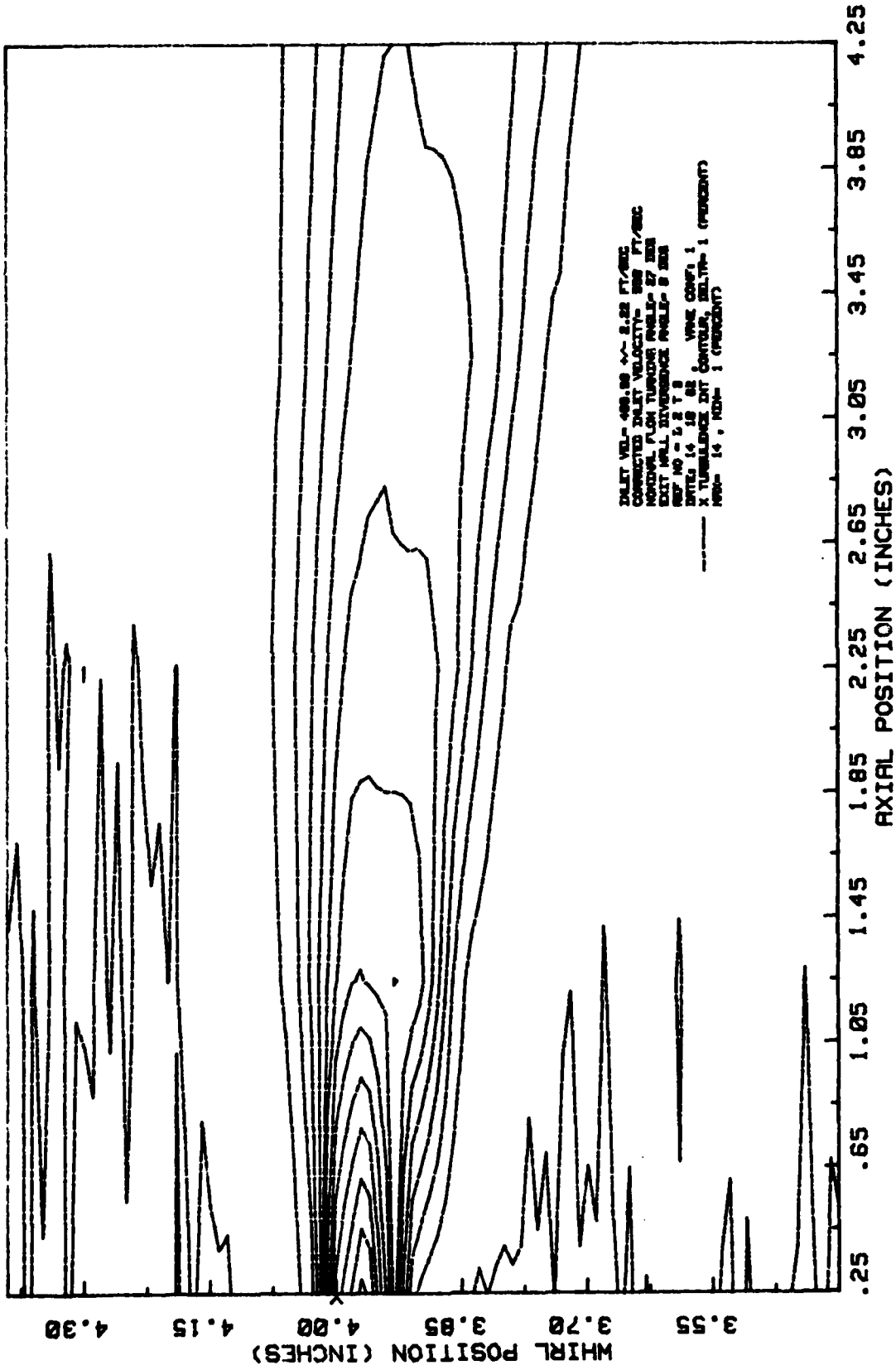

(c) X Turbulence Intensity Contours

Figure 10.-Continued.

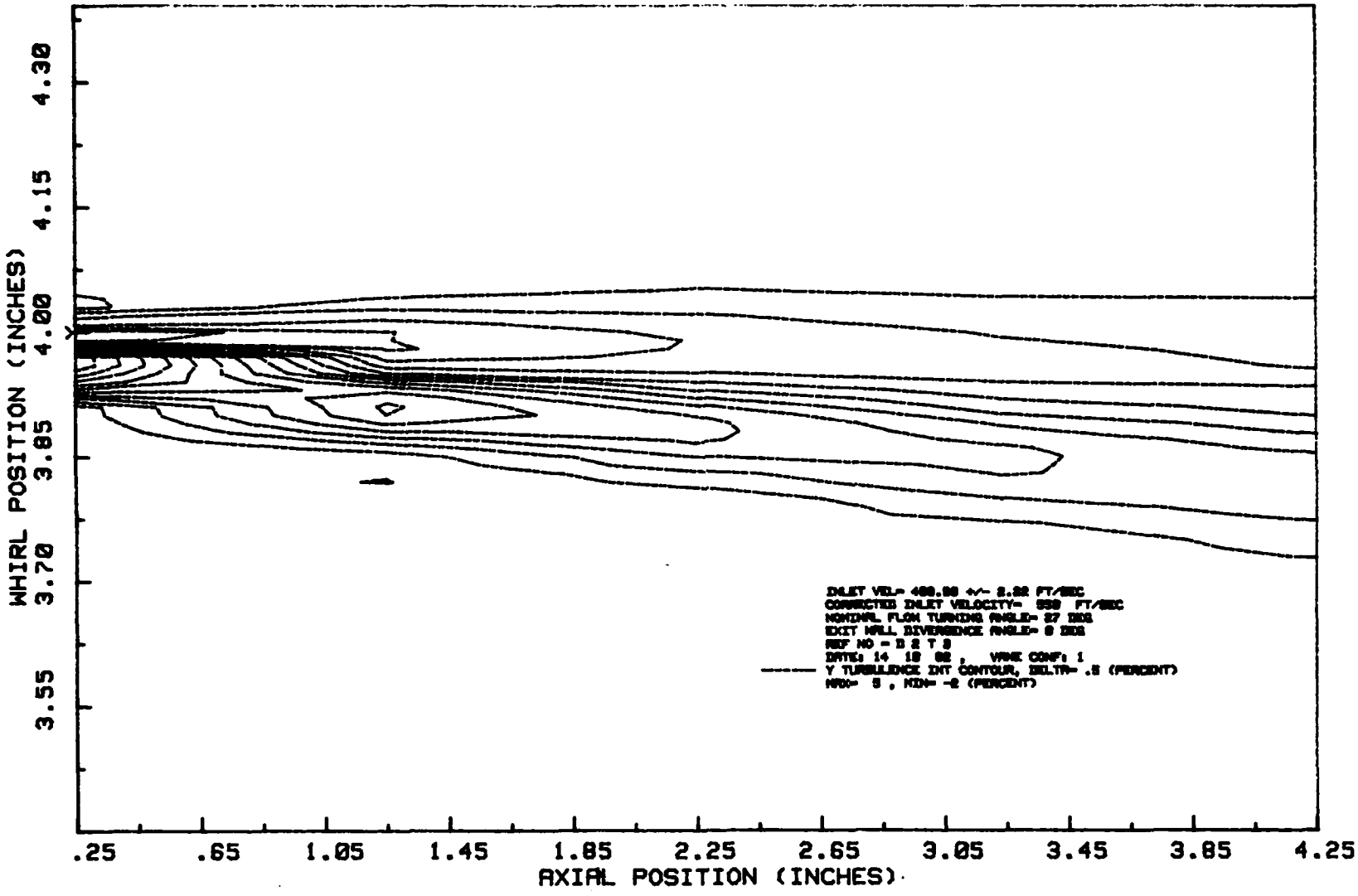

(d) Y Turbulence Intensity Contours

Figure 10.-Concluded

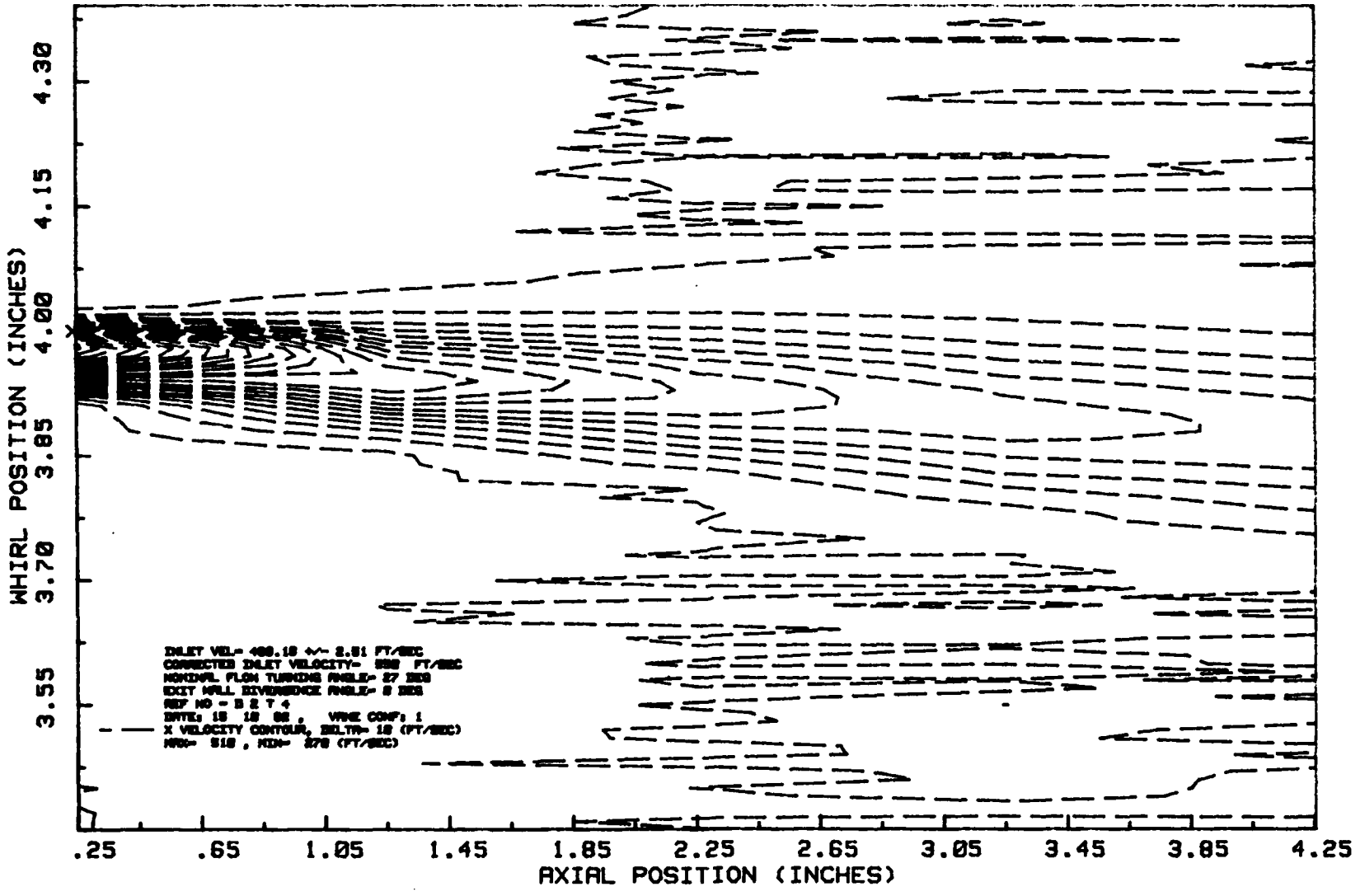

(a) X Velocity Contours

Figure 11. Smooth Vanes Test No 2 Velocity and Turbulence Intensity Contours.

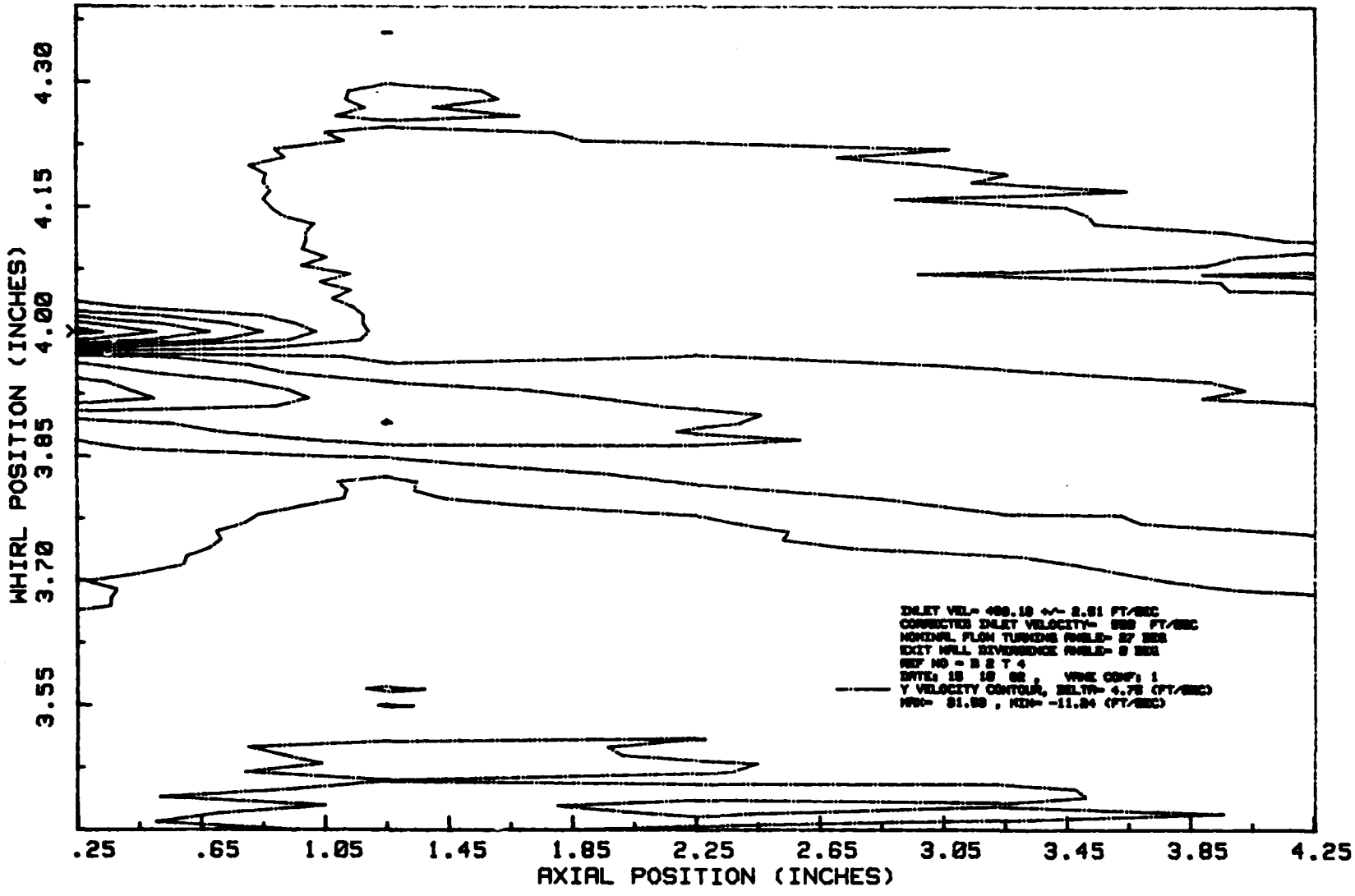

(b) Y Velocity Contours

Figure 11.-Continued.

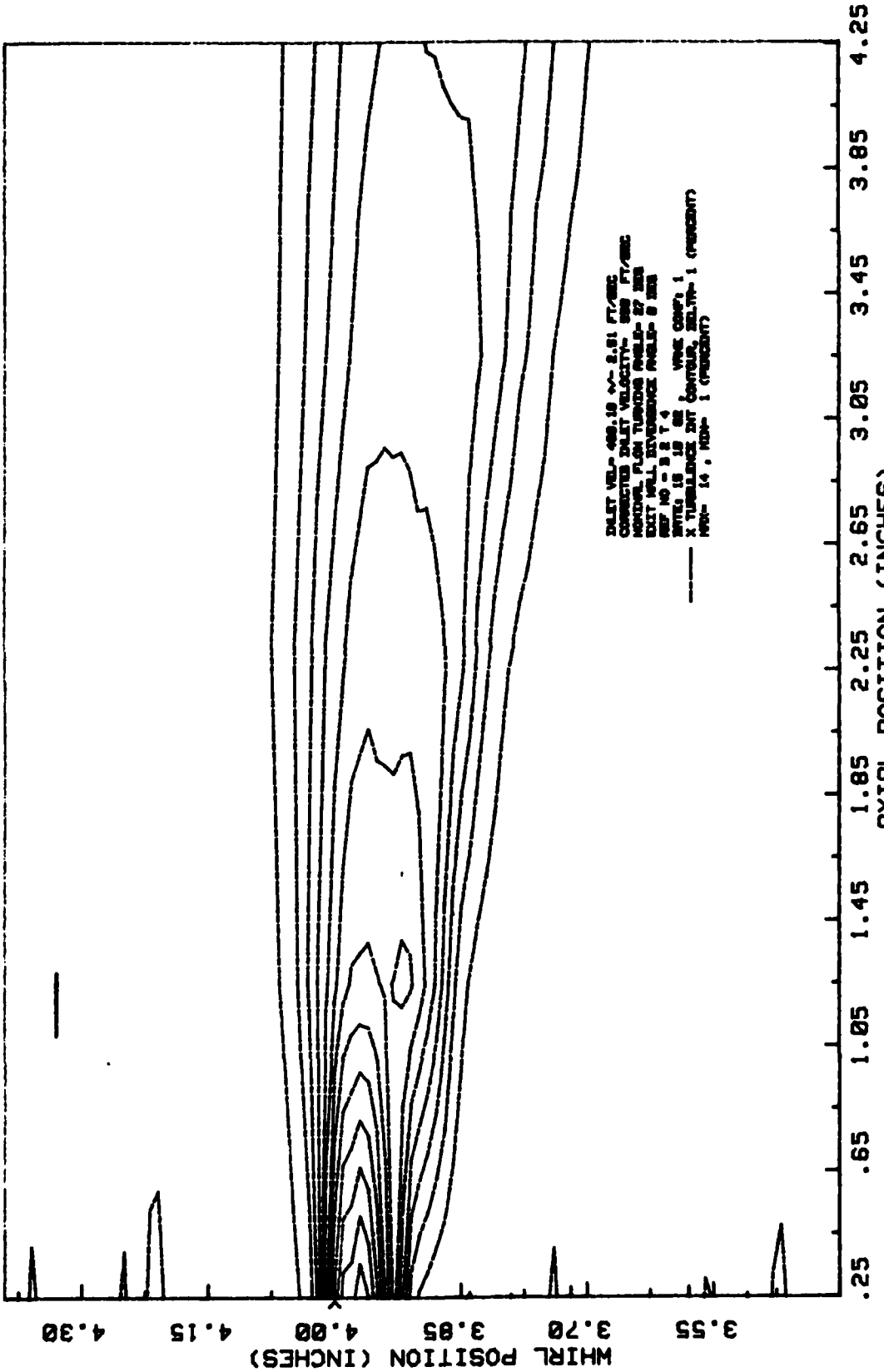

(c) X Turbulence Intensity Contours

Figure 11.-Continued.

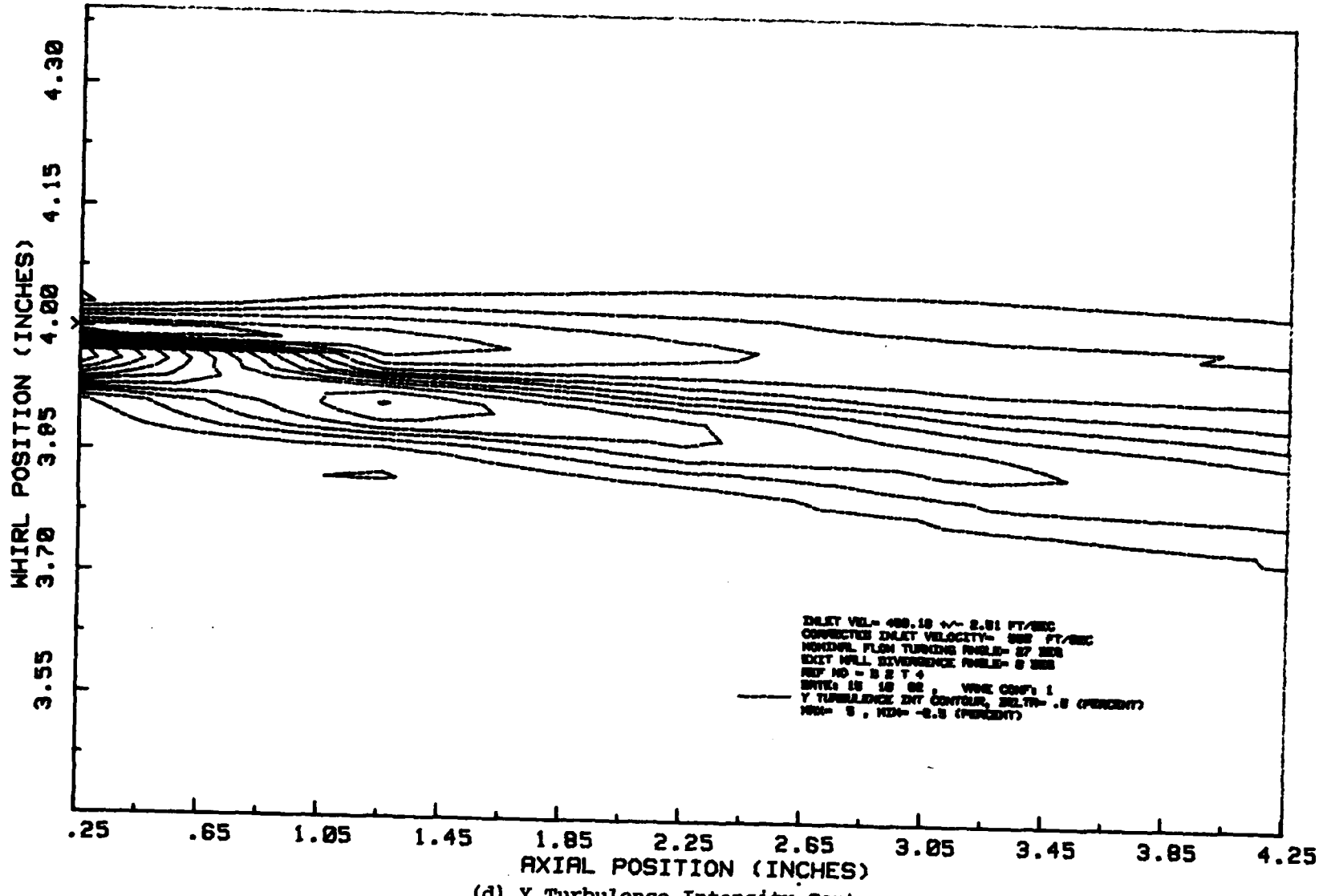

(d) Y Turbulence Intensity Contours

Figure 11.-Concluded.

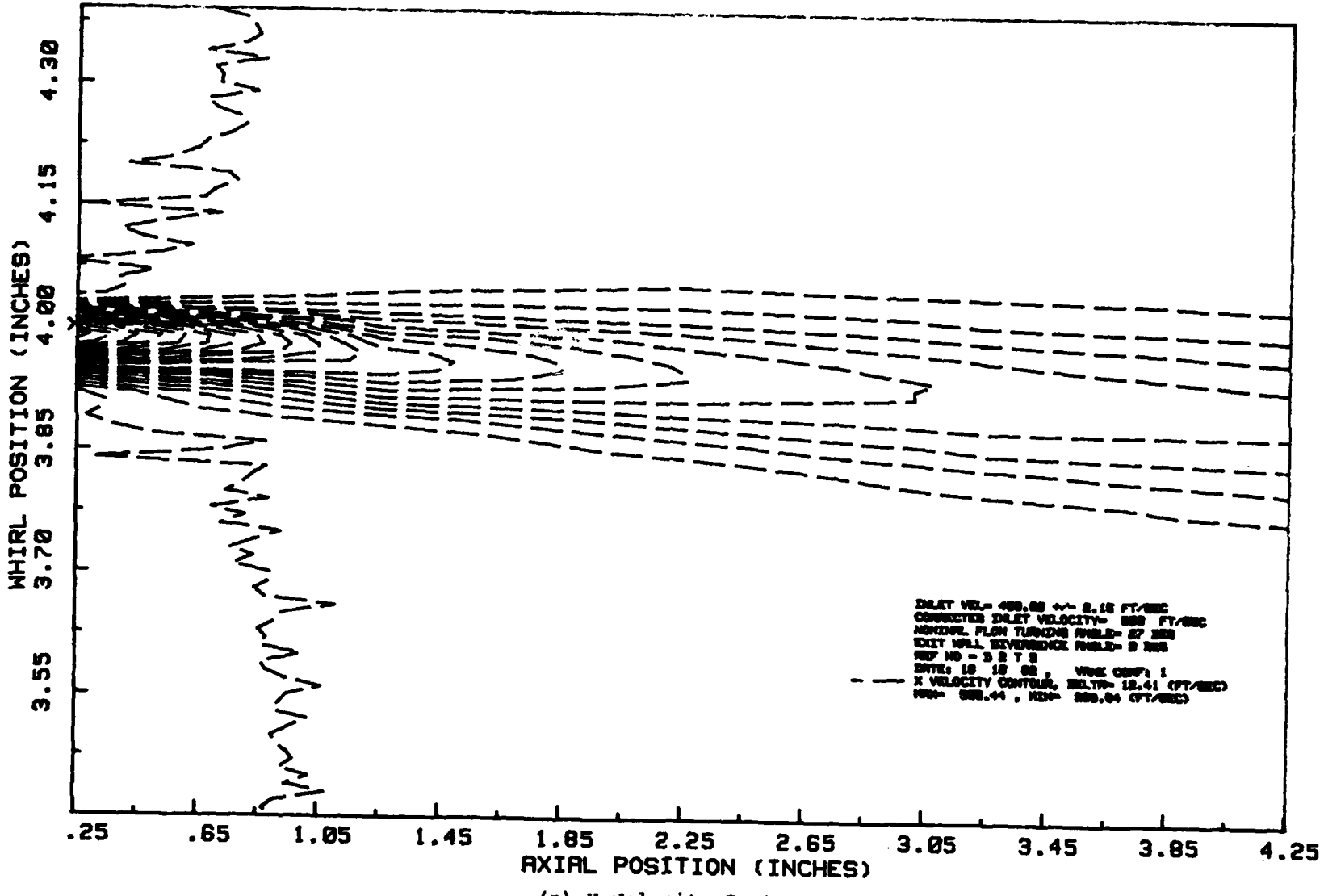

(a) X Velocity Contours

Figure 12. Rough Vanes Velocity and Turbulence Intensity Contours.

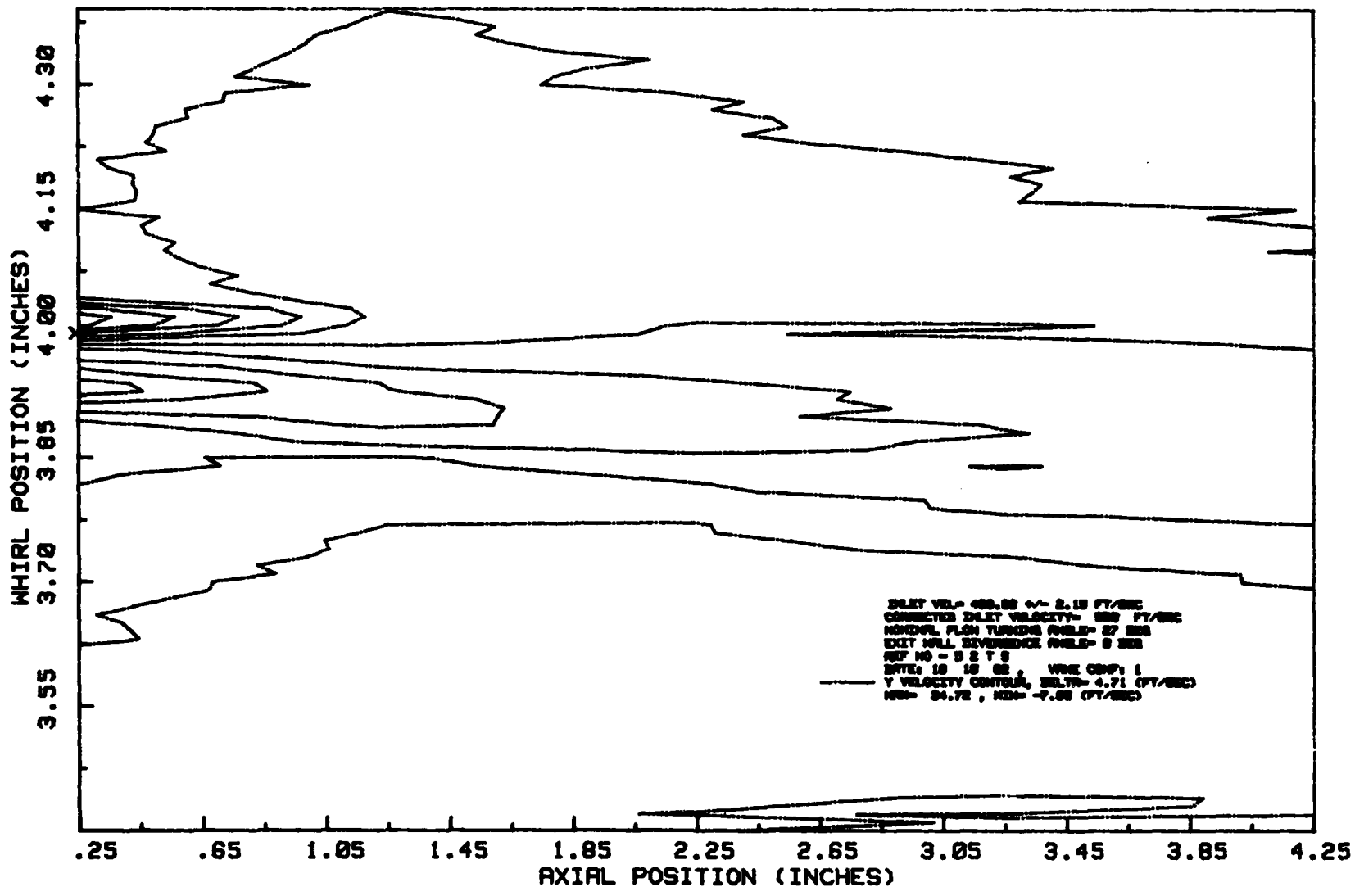

(b) Y Velocity Contours

Figure 12.-Continued.

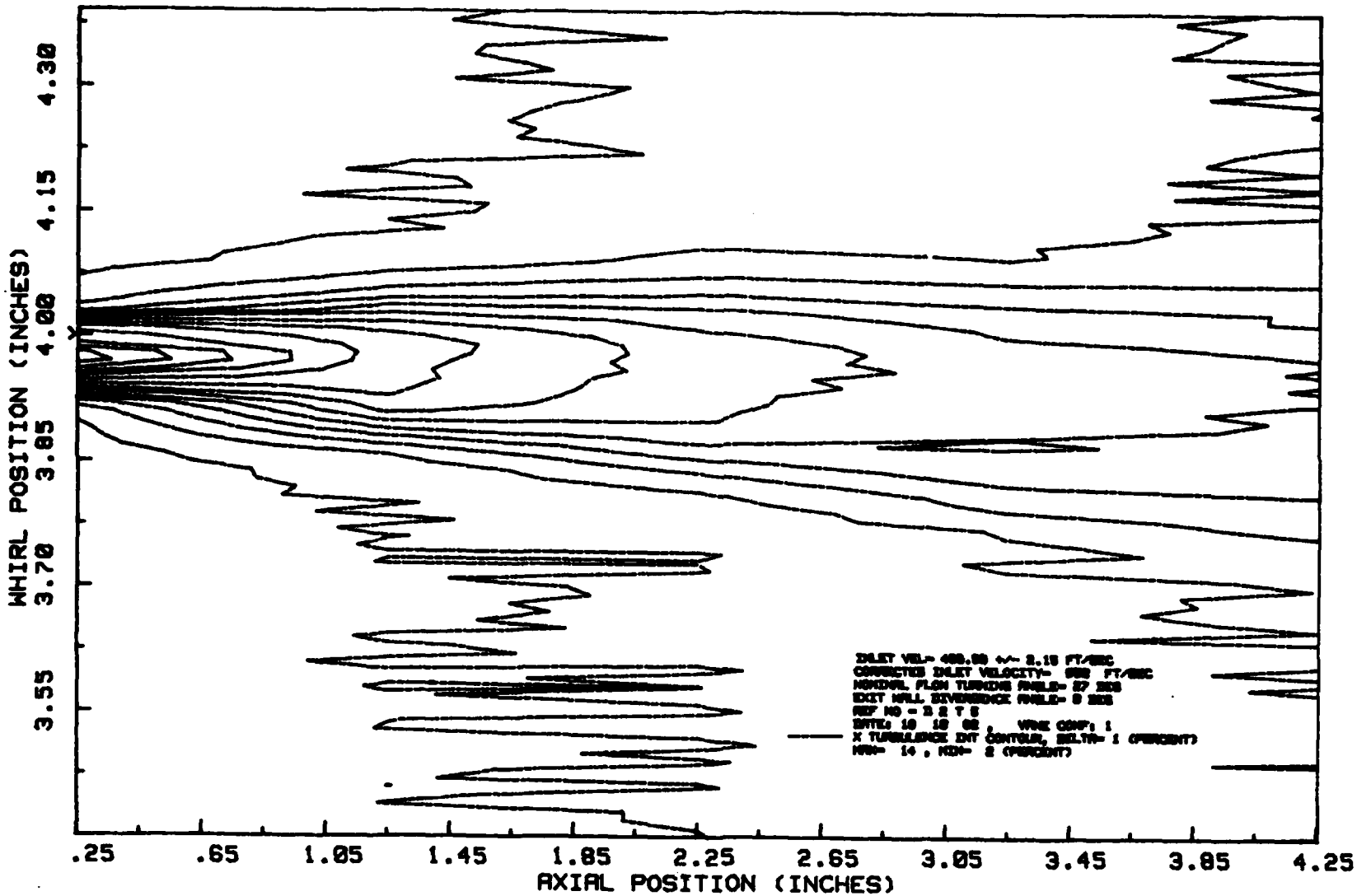

(c) X Turbulence Intensity Contours

Figure 12.-Continued.

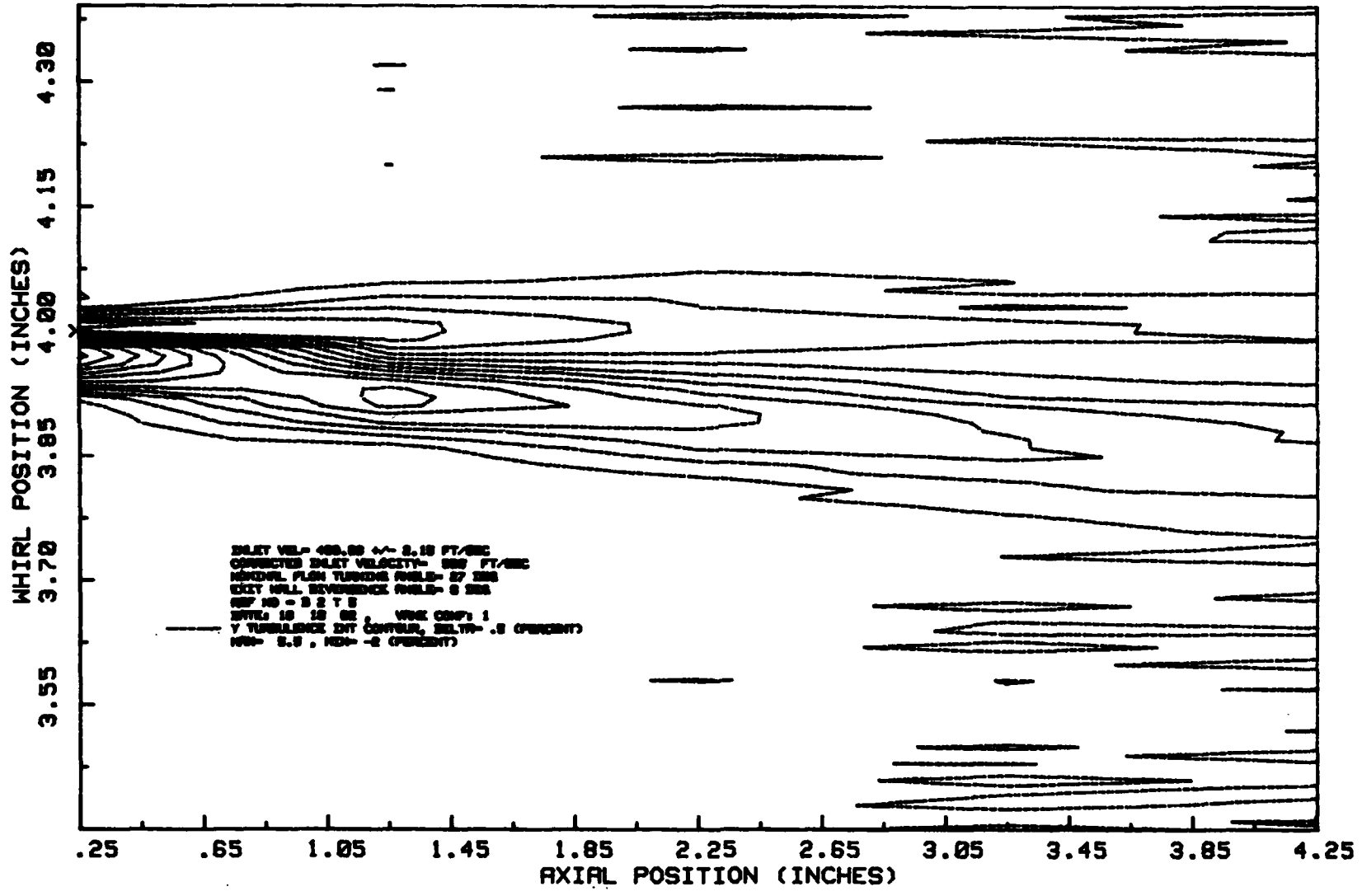

(d) Y Turbulence Intensity Contours

Figure 12.-Concluded.

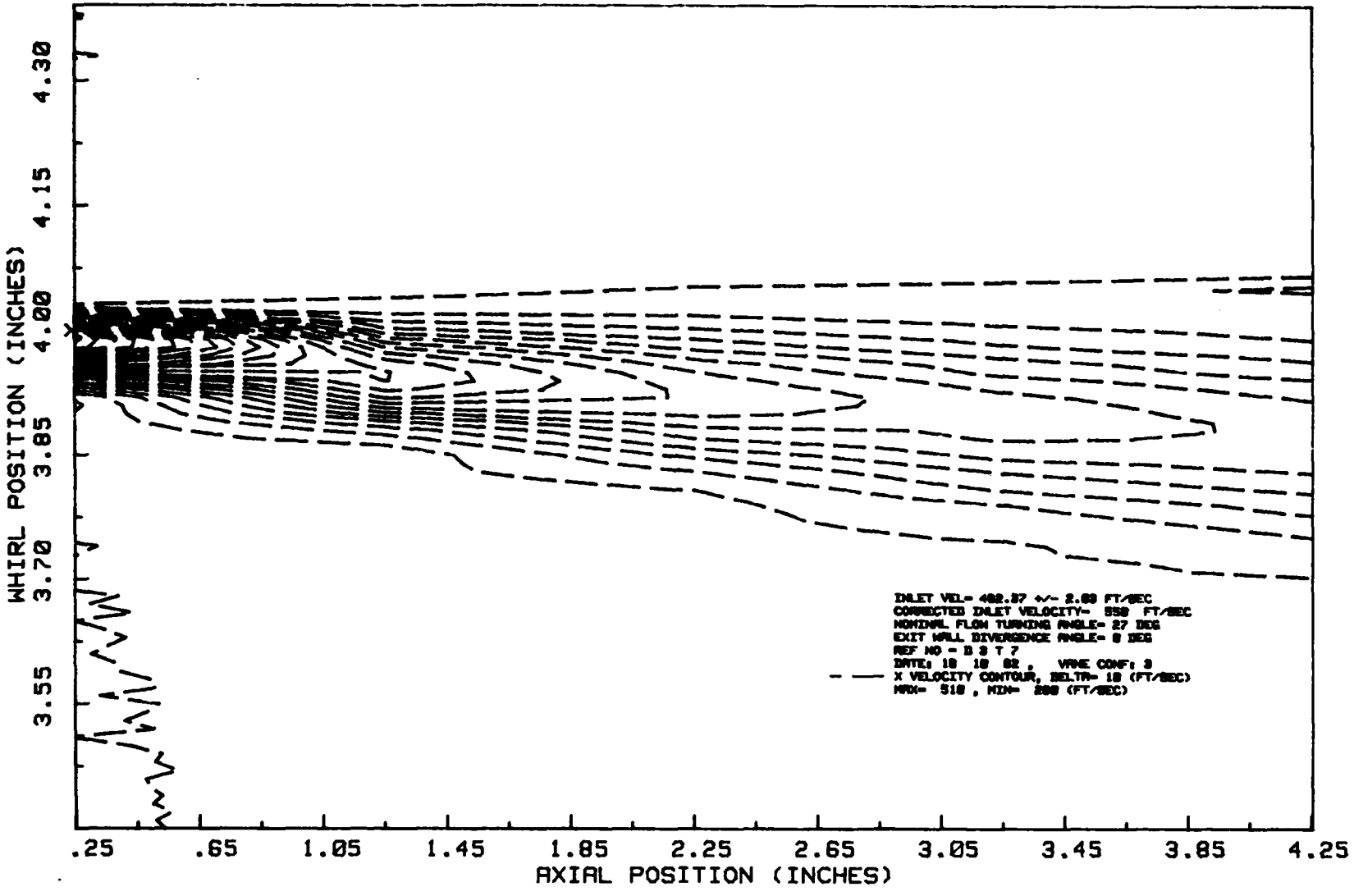

(a) X Velocity Contours

Figure 13. Rough Pressure Side Vanes Velocity and Turbulence Intensity Contours.

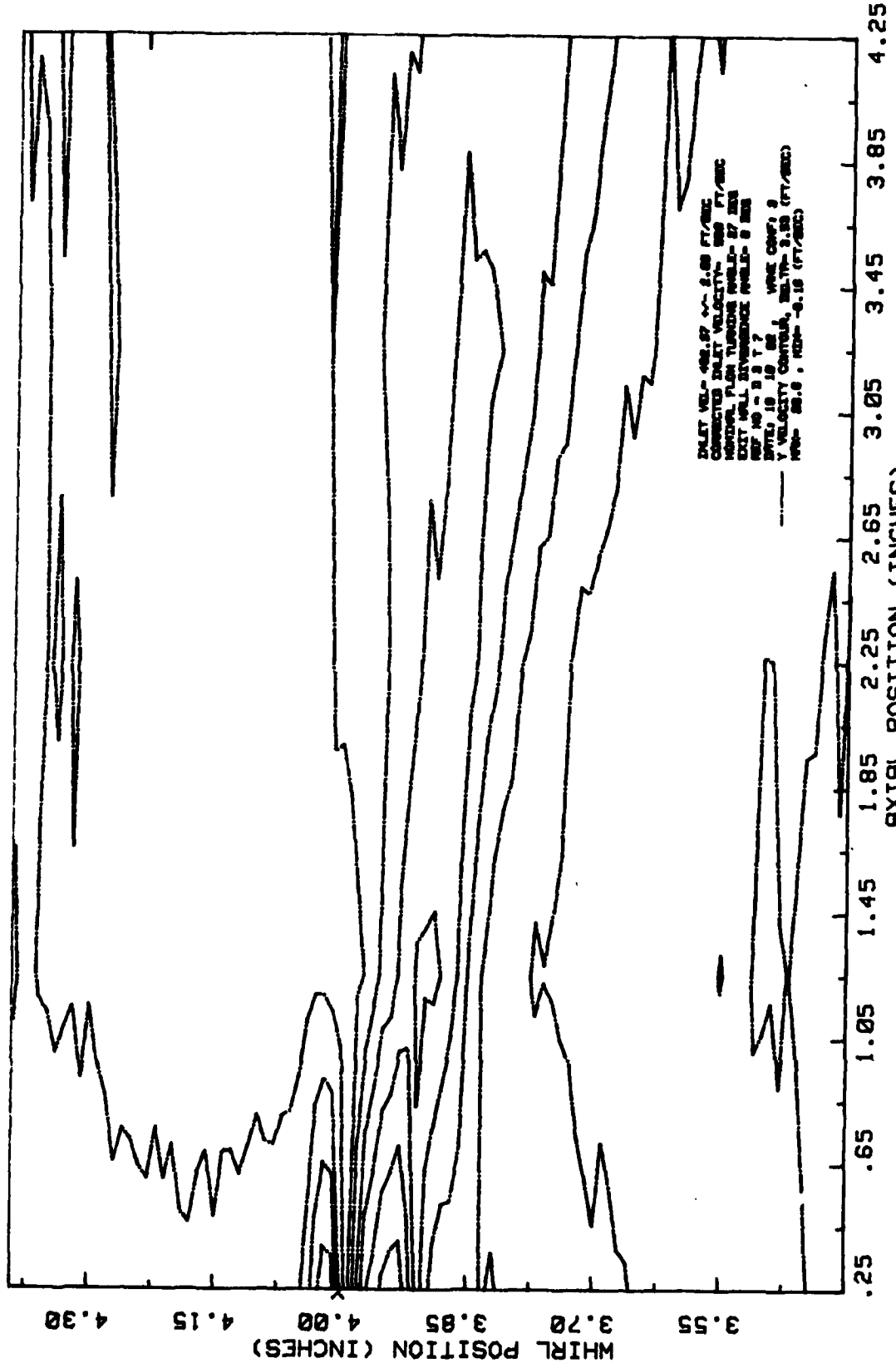

(b) Y Velocity Contours

Figure 13.-Continued.

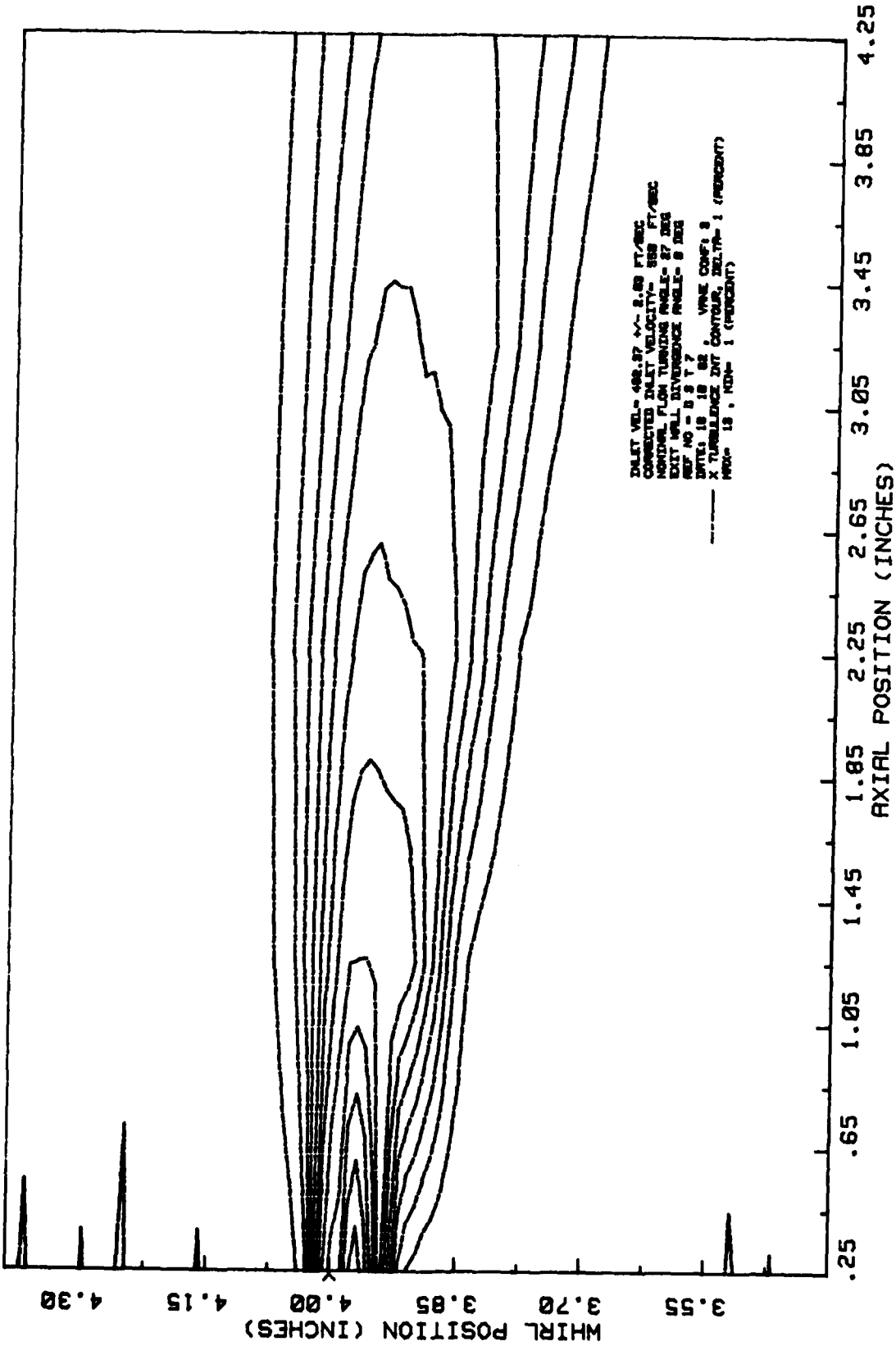

(c) X Turbulence Intensity Contours

Figure 13.-Continued.

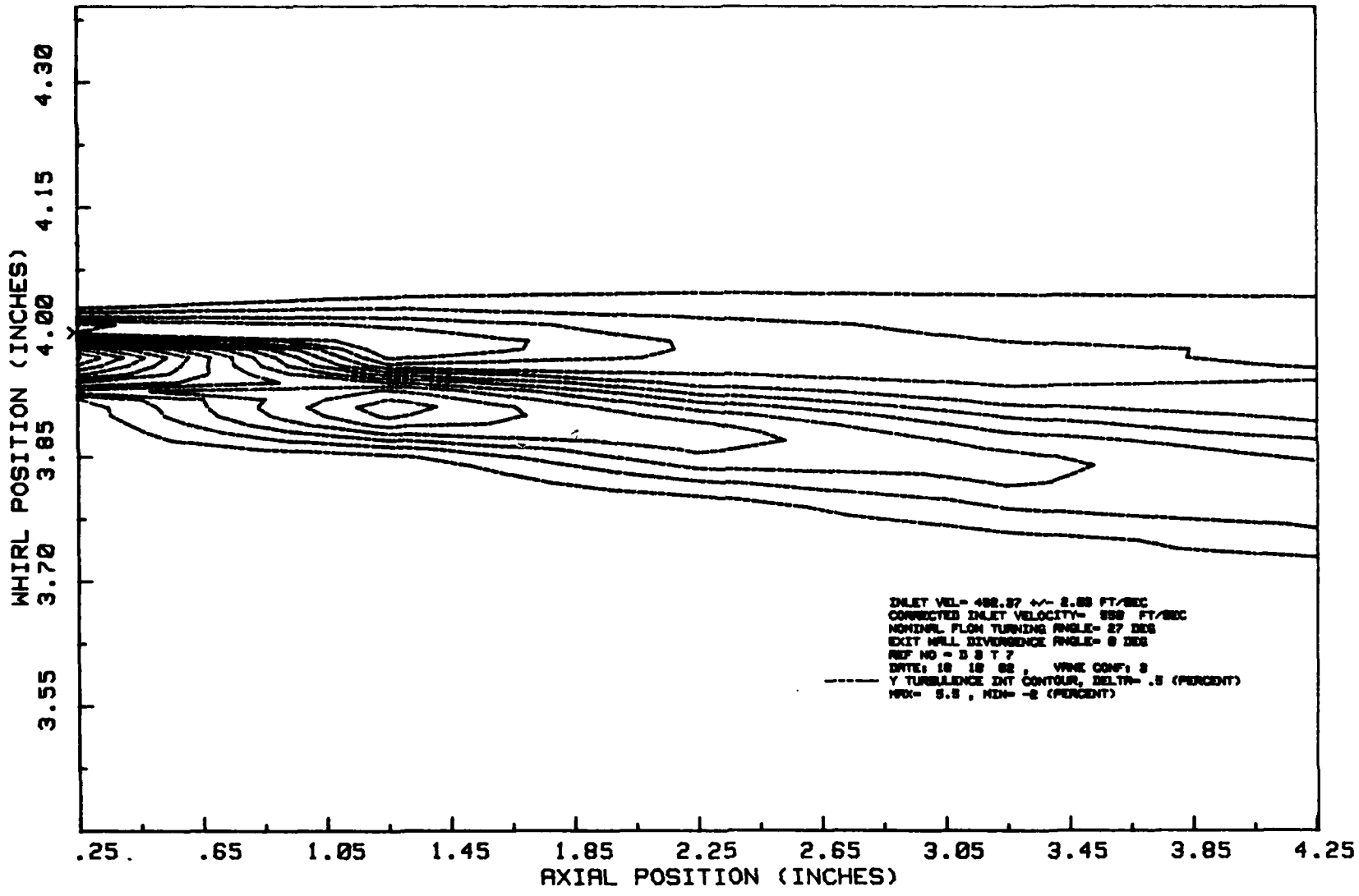

(d) Y Turbulence Intensity Contours

Figure 13.-Concluded.

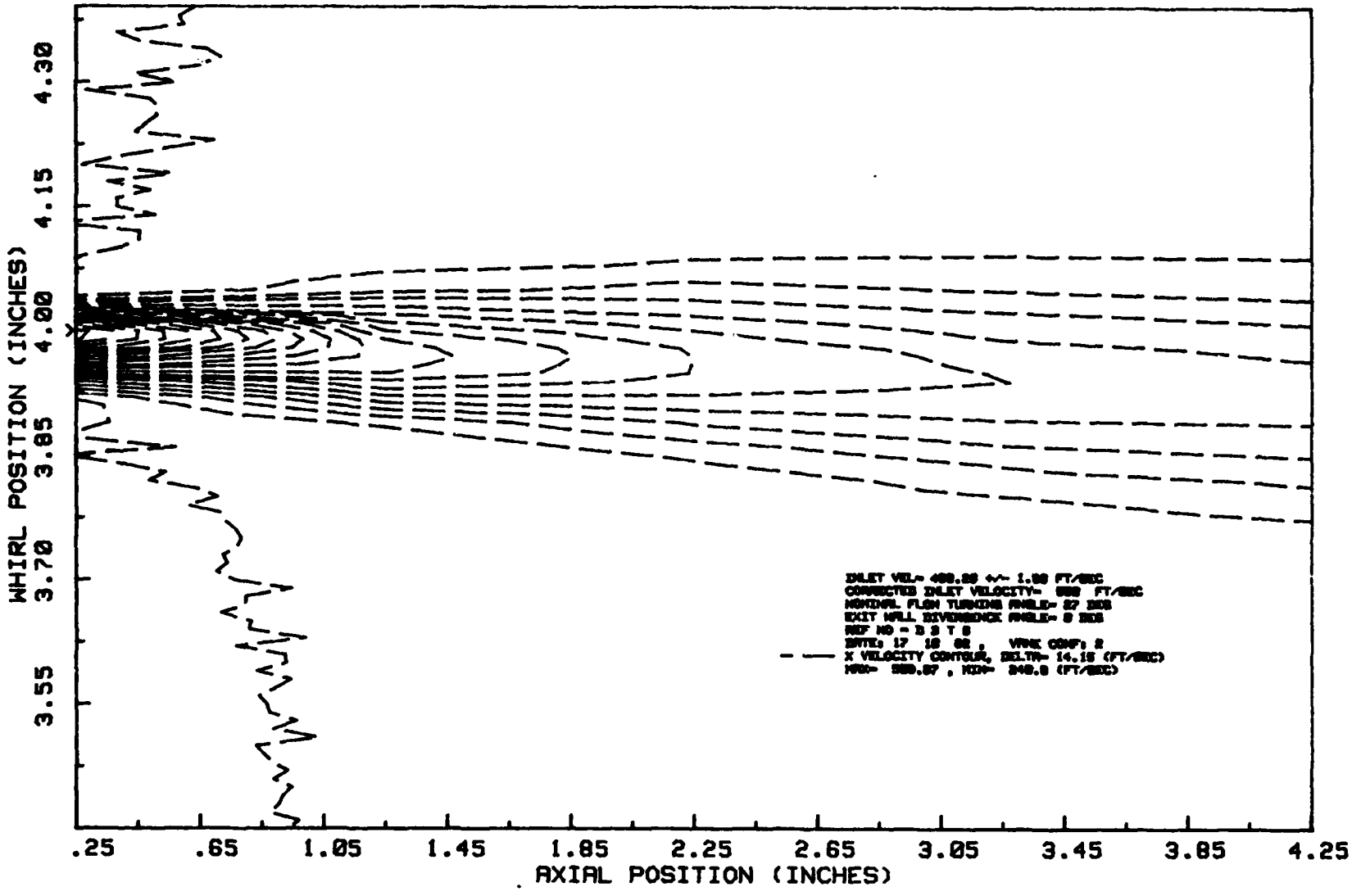

(a) X Velocity Contours

Figure 14. Rough Suction Side Vanes Velocity and Turbulence Intensity Contours.

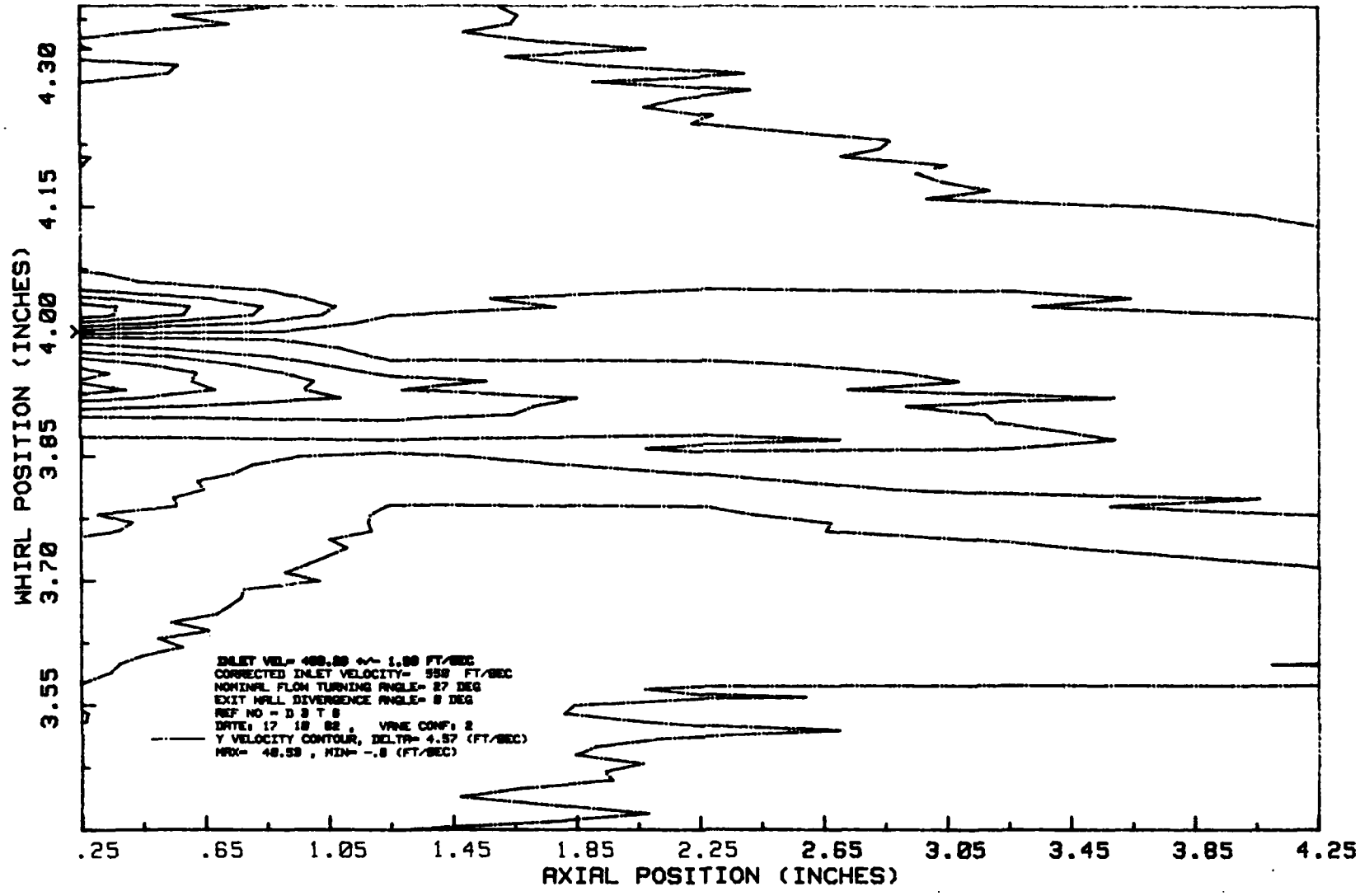

(b) Y Velocity Contours

Figure 14.-Continued.

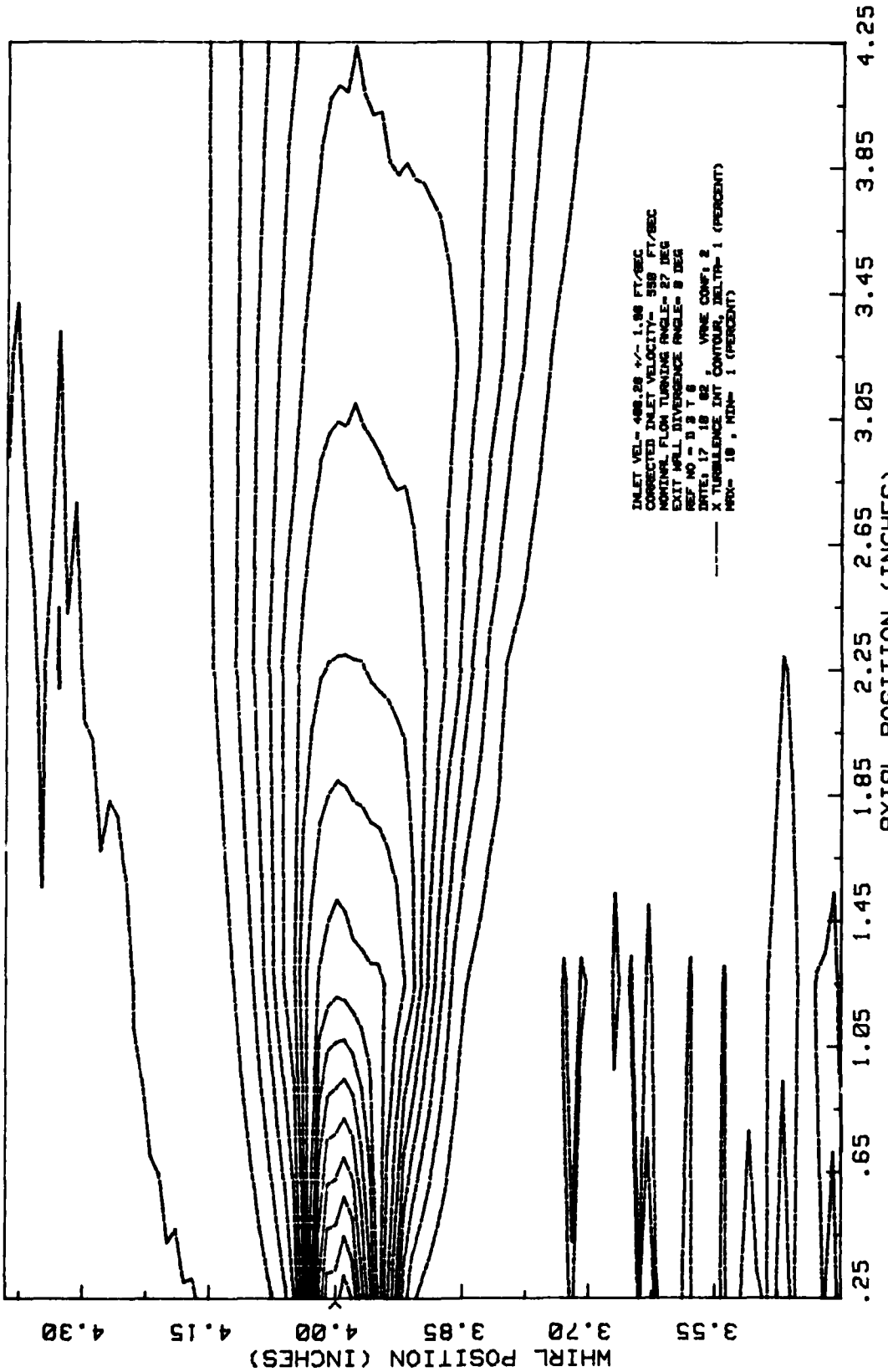

(c) X Turbulence Intensity Contours

Figure 14.-Continued.

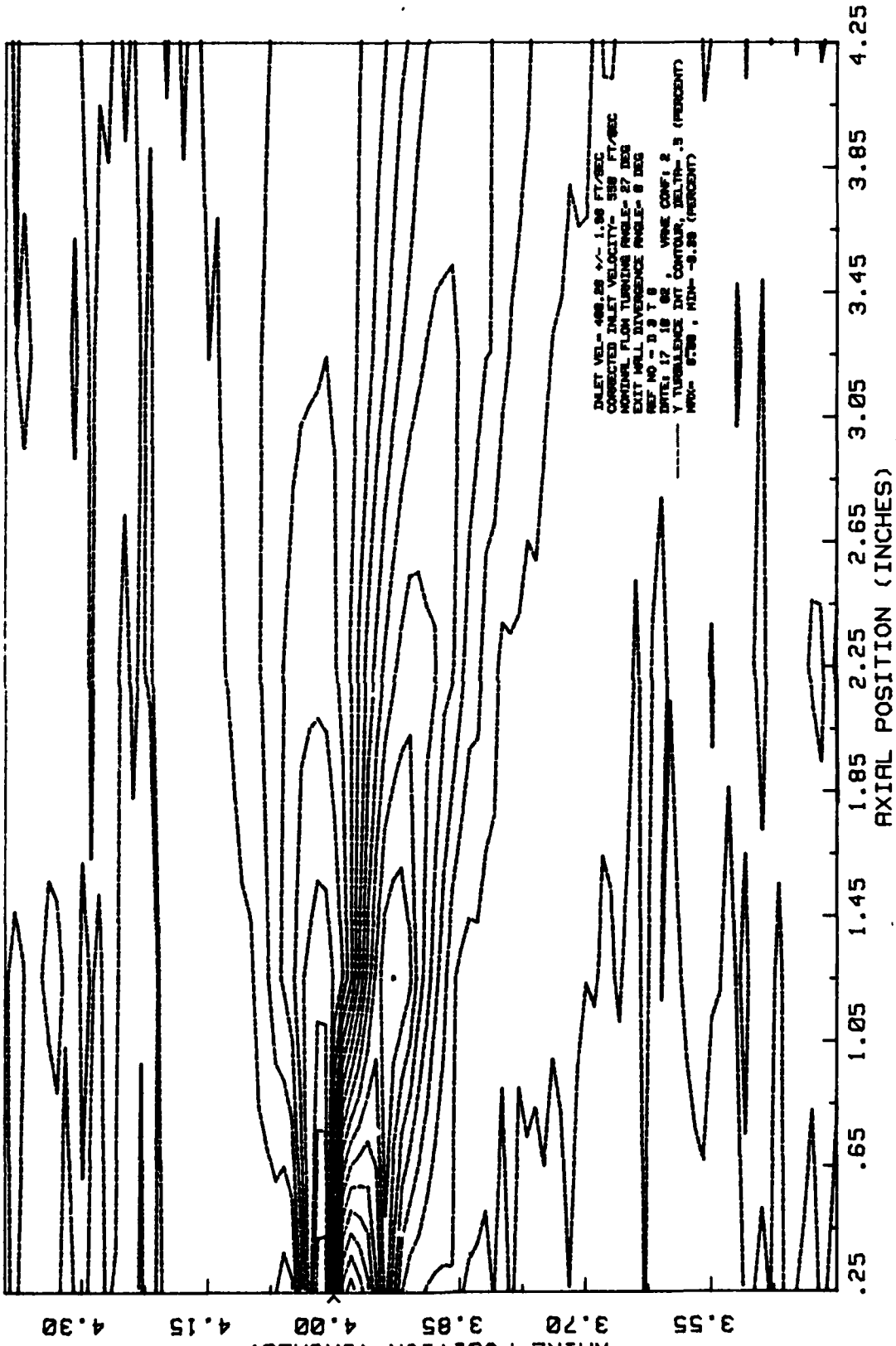

(d) Y Turbulence Intensity Contours

Figure 14.-Concluded.

Vita

David Taylor Genovese was born on 26 February 1956 in Plymouth Massachusetts. After graduating from Plymouth-Carver Regional High School in 1974, he attended Norwich University from which he received the degree of Bachelor of Science in Mechanical Engineering in May 1978. He received his commission in the United States Air Force through the Reserve Officers Training Corps. In August of 1978 he was assigned to the Propulsion Management Division of the San Antonio Air Logistics Center at Kelly Air Force Base Texas. As a project engineer, he provided engineering support for the engines on C-130 and UH-1N aircraft. He later became Lead Engineer and subsequently the Engineering Program Manager for the C-5A aircraft propulsion system. He then served as Aide to the Commander of the Air Logistics Center until entering the School of Engineering, Air Force Institute of Technology, Wright-Patterson AFB, Ohio in May 1981.

UNCLASSIFIED

SECURITY CLASSIFICATION OF THIS PAGE (When Data Entered)

REPORT DOCUMENTATION PAGE	READ INSTRUCTIONS BEFORE COMPLETING FORM
1. REPORT NUMBER: AFIT/GAE/AA/82D-11	2. GOVT ACCESSION NO. A124 688 / 3. RECIPIENT'S CATALOG NUMBER
4. TITLE (and Subtitle): ROUGHNESS EFFECTS ON COMPRESSOR OUTLET GUIDE VANES AT HIGH REYNOLDS NUMBER AND HIGH TURNING ANGLE	5. TYPE OF REPORT & PERIOD COVERED: MS THESIS 6. PERFORMING ORG. REPORT NUMBER
7. AUTHOR(s): David T. Genovese, Captain	8. CONTRACT OR GRANT NUMBER(s)
9. PERFORMING ORGANIZATION NAME AND ADDRESS: Air Force Institute of Technology (AFIT-EN), Wright-Patterson AFB, Ohio 45433	10. PROGRAM ELEMENT, PROJECT, TASK AREA & WORK UNIT NUMBERS
11. CONTROLLING OFFICE NAME AND ADDRESS	12. REPORT DATE: December 1982 13. NUMBER OF PAGES: 85
14. MONITORING AGENCY NAME & ADDRESS(if different from Controlling Office)	15. SECURITY CLASS. (of this report): UNCLASSIFIED 15a. DECLASSIFICATION/DOWNGRADING SCHEDULE

16. DISTRIBUTION STATEMENT (of this Report)

Approved for public release; distribution unlimited

17. DISTRIBUTION STATEMENT (of the abstract entered in Block 20, if different from Report)

18. SUPPLEMENTARY NOTES

Approved for public release: IAW AFR 190-17.

LYNN E. WOLAVER

Dean for Research and Professional Development

Air Force Institute of Technology (AIC)

Wright-Patterson AFB OH 45433

19. KEY WORDS (Continue on reverse side if necessary and identify by block number)

Cascade Testing
Compressor outlet guide vanes
High reynolds number
Roughness effects

20. ABSTRACT (Continue on reverse side if necessary and identify by block number)

An experimental investigation of the effects of surface roughness on flow at high Reynolds number over compressor outlet guide vanes at high turning angle in a 2-D cascade was conducted at the Air Force Institute of Technology Cascade Test Facility. A NACA 64 series airfoil with a design lift coefficient of 0.9 and a thickness of 5.5 percent was tested at a solidity of 1.5 and a 27 degree angle of attack.

Two models of roughness were tested: one smoother and one rougher than

DD FORM 1 JAN 73 1473 EDITION OF 1 NOV 65 IS OBSOLETE

UNCLASSIFIED

SECURITY CLASSIFICATION OF THIS PAGE (When Data Entered)

actual compressor vanes. Four configurations of roughness were evaluated: pressure and suction sides smooth, pressure and suction sides rough, pressure side rough with the suction side smooth and suction side rough with the pressure side smooth.

Hot film sensor anemometery was used to determine the velocity and turbulence intensity in the flow field behind the vanes. The section coefficient of drag was calculated based on momentum deficit theory.

Roughness was determined to effect the flow through an increase in the coefficient of drag and changes to the magnitude and profiles of the velocity and turbulence intensity. The greatest effect was caused by roughness on the suction side of the vane with a smooth pressure surface.